Univerzita Karlova v Praze
Matematicko-fyzikální fakulta

DIPLOMOVÁ PRÁCE

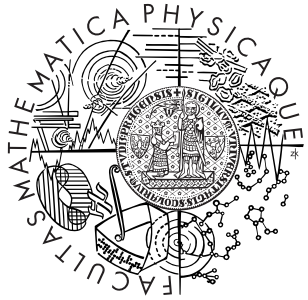

Jiří Kaštil

Vliv substitucí na magnetokalorický jev u vybraných sloučenin vzácných zemin

Katedra fyziky kondenzovaných látek

Vedoucí diplomové práce: Doc. Mgr. Pavel Javorský, Dr.

Studijní program: Fyzika kondenzovaných soustav a materiálů.

2009

Děkuji Doc. Pavlu Javorskému za jeho ochotu, trpělivost a rady, které mi poskytl při měření a tvorbě mé diplomové práce. Konzultace s Doc. Pavlem Javorským byly vždy podnětné a motivující. Zároveň mu děkuji za vydatnou pomoc s jazykovou korekturou mé práce. Děkuji Ing. Jiřímu Kamarádovi za umožnění provedení přímého měření a za jeho vlídný přístup.

Prohlašuji, že jsem svou diplomovou práci napsal samostatně a výhradně s použitím citovaných pramenů. Souhlasím se zapůjčováním práce.

V Praze dne 14.4.2009 Jiří Kaštil

Contents

Název práce: Vliv substitucí na magnetokalorický jev u vybraných sloučenin vzácných zemin
Autor: Jiří Kaštil
Katedra: fyziky kondenzovaných látek
Vedoucí bakalářské práce: Doc. Mgr. Pavel Javorský, Dr.
e-mail vedoucího: javor@mag.mff.cuni.cz

Abstrakt: V práci byla studována anizotropie magnetokalorického jevu na monokrystalu sloučeniny DyNiAl. Naměřená data ukázala silnou anizotropii magnetokalorického jevu. Maximum magnetokalorického jevu se objevilo při orientaci podél osy c, zatím co při kolmé orientaci vzorku byla změna entropie velmi malá. Vliv substitucí na magnetokalorický jev byl studován na sloučeninách $Gd(Co_{1-x}Rh_x)_2$ (kde x bylo mezi 0.05 a 0.30) a na sloučeninách $Dy(Co_{1-x}Fe_x)_2$ (kde x bylo mezi 0.00 a 0.03). Náhrada Co za Rh vedla k poklesu teploty přechodu T_c. Maximum změny entropie mírně rostlo s rostoucím obsahem Rh. Pro substituci Fe za Co T_c prudce rostla, zatím co maximum změny entropie velmi rychle klesalo. Poslední ze studovaných systémů byly slitiny $Gd_{1-x}Tb_x$ (kde x bylo mezi 0.00 a 0.40). Byl měřen vliv tvaru a orientace vzorku na magnetokalorický jev. Největší změna entropie byla naměřena na tenkém pásku orientovaném podél pole. Při určování magnetokalorického jevu byly použity tři měřící techniky: měření tepelné kapacity, měření magnetizace a přímé měření změny teploty.

Klíčová slova: magnetokalorický jev, DyNiAl, substituce, slitina $Gd_{1-x}Tb_x$

Title: The influence of substitutions on the magnetocaloric effect in selected rare-earth compounds
Author: Jiří Kaštil
Department: of Condensed Matter Physics
Supervisor: Doc. Mgr. Pavel Javorský, Dr.
Supervisor's e-mail address: javor@mag.mff.cuni.cz

Abstract: The anisotropy of the magnetocaloric effect was studied on DyNiAl single crystal. Our data reveal a strong anisotropy of the magnetocaloric effect. The large effect occurs for field applied along the c-axis whereas the entropy change is small for the perpendicular field direction. The influence of substitution on the magnetocaloric effect was measured in the $Gd(Co_{1-x}Rh_x)_2$ compounds (where x was from 0.05 to 0.30) and $Dy(Co_{1-x}Fe_x)_2$ compounds (where x was from 0.00 to 0.03). The substitution of Co by Rh leads to a decrease of the transition temperature, T_c, and increase of the maximum entropy change. The T_c increases but the maximum of entropy change quickly decreases in case of Fe substitution. The last studied systems were the $Gd_{1-x}Tb_x$ alloys with x in range from 0.00 to 0.40. The influence of the sample shape and orientation was studied. The thin ribbon oriented along the magnetic filed gave the highest value of the entropy change. The three measurement techniques were used: the heat capacity measurement, the magnetization measurement and the direct measurement of the temperature change.

Keywords: magnetocaloric effect, DyNiAl, substitution, $Gd_{1-x}Tb_x$ alloys

Chapter 1

Introduction

1.1 Magnetocaloric effect

The magnetocaloric effect (MCE) is among the most fundamental physical properties of magnetic solids. This intrinsic property is defined as the adiabatic temperature change or the isothermal entropy change of materials when varying external magnetic field. Both the sign and the extent of the temperature or entropy change between the initial and final state of the material dependent on numerous intrinsic and extrinsic factors. The magnetocaloric effect was first observed by Emil Warburg in 1881 on the iron samples. The cooling method of adiabatic demagnetization which allows reach the ultra low temperature was developed in 1920s. This method was independently developed by Debye (1926) and Giauque (1927). A few years later, in 1933, W. F. Giauque and D. P. MacDougall performed an experiment at which they reach 0.25 K [1]. The Nobel price was given to the W. F. Giauque in 1949 among others for the research of magnetocaloric effect.

1.2 General motivation

Magnetic cooling technique is now considered as a serious alternative for conventional refrigeration. Materials displaying large MCE are studied intensively during last years. One of the first functioning room-temperature cooling device was shown in 1997 and the working material was Gd which is still one of the most suitable materials. The materials with a large magnetocaloric effect are mostly the rare-earth intermetallic compounds like e.g. $Gd_5Ge_2Si_2$ [2–4] and $La(Fe_{1-x}Si_x)_{13}$ [5–7]. Among other systems, we should mention for example $MnFeP_{0.5}Ge_{0.5-x}Si_x$ [8], $MnAs_{1-x}Sb_x$ [9] and FeRh [10]. Although the mentioned materials exhibit large magnetocaloric effect, there are difficulties when considered the real application. The magnetocaloric effect of the FeRh is irreversible and disappear after first application of the magnetic field for example.

Materials with the large magnetocaloric effect are potential candidates for a real ap-

plication, but on the other hand, the study of the magnetocaloric effect can lead to the deeper understanding of the magnetic interactions, phase transitions and other microscopic properties of the material. The measurement of the material which exhibits only a small magnetocaloric effect or magnetocaloric effect reaches maximum at low temperatures is still meaningful and valuable.

In this work we present results of the experimental study of the magnetocaloric effect in three types of materials. We measured the DyNiAl compound, substituted $RECo_2$ compounds and the Gd-Tb alloys.

DyNiAl belongs to a large group of rare-earth intermetallics crystallizing in the hexagonal ZrNiAl-type structure. The RENiAl compounds show complex magnetic order at low temperatures with two magnetic phases when RE = Sm, Gd, Tb, Dy, Ho or Tm [11, 12]. The second phase transition occurs here at about one half of the ordering temperature, $T_1 \approx \frac{T_C}{2}$, what can be favorable for magnetocaloric effect. The magnetocaloric effect on polycrystalline TbNiAl [13], HoNiAl [14] and DyNiAl [15] was already studied and showed interesting characteristics. We focus on a rarely discussed aspect of MCE - the anisotropy of the magnetocaloric properties. The use of intrinsic anisotropic properties is one of the promising ways to increase the refrigerant capacity of a given material and has been theoretically and experimentally studied [16–18].

The second studied system are the $RECo_2$ compounds. The magnetic and magnetocaloric properties of $RECo_2$ compounds are strongly influenced by substitutions of Co by other elements. The magnetocaloric effect in many systems with substituted Co atoms has been studied in recent years (e.g. [19–23]). In this work, we aim to modify the transition temperature of $DyCo_2$ and $GdCo_2$ compounds toward the range between 200 and 300 K by two different substitution. We use iron in $DyCo_2$ and rhodium in $GdCo_2$.

The last system presented in this thesis are the Gd-Tb alloys. The Gd-Tb alloys are considered as a real working material in a prototype magnetocaloric cooling device constructed in cooperation between our department and the Faculty of Mechanical Engineering at Czech Technical University in Prague. Therefore, beside the characteristic of the magnetocaloric effect, we investigate some more technical problems like the influence of the sample shape. The different measurement techniques were used on this system and the obtained results are discussed.

1.3 How to read this work

I divide this work in several chapters. Short introduction had to acquaint the reader with the subject of this work and give the foundation of the research.

The required theory can be find in the next chapter which consist from tree parts. The first part represents the short overview of the origin of the magnetism and of the magnetic interactions mainly in the RE-T systems where the RE is the rare-earth and T

is the transition metal. The basic concept of the magnetocaloric effect and the equations to enumerate the magnetocaloric characteristics from the measurement are presented in the second part and the third part of chapter 2 is given to the influence of substitution on the magnetocaloric effect.

The chapter 3 describes the used experimental techniques. The preparation of the samples is summarized in the first part, the x-ray characterization of the samples in the second part. The last part of the third chapter is dedicated to the measurement techniques of the MCE. The indirect measurement techniques, the magnetization measurement and the heat capacity measurement, are followed by the direct measurement of the temperature change.

The fourth chapter contains the obtained results and the discussion of these results. The chapter is divided in three parts which correspond with the studied systems. First we present the measurement of the DyNiAl single crystal. The second part is given to the $RE\mathrm{Co}_2$ systems and is divided in two parts: $\mathrm{Gd(Rh,Co)}_2$ and $\mathrm{Dy(Fe,Co)}_2$. The results obtained on Gd-Tb alloys are described in the last part of the chapter 4. More attention was given to the $\mathrm{Gd}_{0.9}\mathrm{Tb}_{0.1}$ then to the others concentrations and the results for this concentration are presented in a special part 4.3.1.

The conclusions, as chapter 5 and the list of references are at the end of this work.

Chapter 2

Theoretical background

2.1 Magnetic interactions

Basic quantities to describe the magnetism are the magnetization M, the magnetic field induction B and the intensity of the magnetic field H. The following equation holds:

$$B = \mu_0(H + M), \tag{2.1}$$

where μ_0 is the permeability of the vacuum. The response of the matter on the magnetic field is expressed as

$$M = \chi H, \tag{2.2}$$

where χ is the susceptibility of the matter. Materials with the negative susceptibility are diamagnetic. The materials with the positive susceptibility are paramagnetic or magnetically ordered.

Diamagnetism

Diamagnetism is the aspiration of the electron to shield effect of the magnetic field. When the magnetic field is applied the current is induced according to the Lorentz law. The induced current tries to prevent the change of the magnetic flux. The diamagnetic susceptibility in a real system is very small and is in order of -10^{-13} to -10^{-12} $\mathrm{m^3mol^{-1}}$. The diamagnetic response can be directly seen only on ions with the filled electron shells (Larmor diamagnetism). The diamagnetic materials are for example copper, gold and the rare-gases.

Paramagnetism

Paramagnetism is characterized by a positive susceptibility. The directions of magnetic moments are randomly distributed in zero field in the paramagnetic state. Paramagnetism of the free ions has origin in the spin moment S and the orbital moment L of the ions.

The ground state of the free ions without field is $(2J+1)$-times degenerated and is given by Hunds rule [24] and characterized by the total momentum J.

The magnetic moment of the free ions is given by the following equation:

$$\mu = -g\mu_B J, \tag{2.3}$$

where the μ_B is the Bohr magneton and g is the g-factor which is calculated from the S and L numbers. The applied magnetic field splits the ground state in to $(2J+1)$ equidistant energy levels. The magnetization of the free ions with the total momentum J can be calculated as

$$M = NgJ\mu_B B_J(x), \qquad x \equiv \frac{gJ\mu_B B}{k_B T}. \tag{2.4}$$

The B_J is the Brillouin function and is defined as

$$B_J(x) = \frac{2J+1}{2J} cotgh\left(\frac{(2J+1)x}{2J}\right) - \frac{1}{2J} cotgh\left(\frac{x}{2J}\right). \tag{2.5}$$

The Curie law can be derived for small x from the equation (2.4).

$$\frac{M}{B} = \frac{C}{T} \tag{2.6}$$

Where C is the Curie constant. Such paramagnetic contribution is called Van Vleck paramagnetism.

This calculation holds exactly for the free ions with partially filed electron shell. When the ions is in the solid, the crystal field has to be taken in to account. The 4f shells of the rare-earth ions are well shielded by the 5s and 5p electrons and the previous derivation is correct. The situation is different for the 3d metals. The 3d electrons contribute to the metallic bond and are highly influenced by the crystal field. The crystal field lower the degeneracy of the ground state and leads to the so called freezing of the orbital momentum. The L number has to be taken as zero and only the spin S plays a role.

Another paramagnetic contribution comes from the free electrons. Pauli showed [24] that the use of the Fermi-Dirac distribution function leads to the temperature independent magnetization of the free electrons:

$$M \approx \frac{N\mu^2 B}{k_B T_F}, \tag{2.7}$$

where N is the number of atoms in unit volume, k_B is the Boltzman constant and T_F is the Fermi temperature. This paramagnetic contribution to the total susceptibility is only a fraction of the Van Vleck paramagnetism.

Magnetic ordering

The magnetic ordering in the material originates from the mutual interactions between magnetic moments. The magnetic ordering arise when the interaction exceed the random thermal motion. The exchange interaction is the most prominent interaction in magnetic materials. The exchange interaction can be of different type depending on the material. The three basic types of exchange interactions are the direct exchange interaction, the indirect exchange interaction and the indirect exchange interaction of RKKY type. The direct exchange interaction acts directly on the neighboring magnetic atoms. The indirect exchange interaction uses the nonmagnetic atom as a mediator. The magnetic moment interact through the itinerant electrons when the RKKY interaction is present. The strength of the exchange interactions can be expressed with help of an internal "exchange field" that works on the magnetic moment and can be in order of 100 T.

The magnetic properties of material depend on the character of the electrons of the solid. In this work we will speak mainly about the *RE*-*T* compounds where T represents the 3d-metal and *RE* stands as lanthanides. The lanthanides is a set of elements placed between lanthanum and lutetium in the Periodic Table of Elements and together with scandium and yttrium create group called rare-earths. The magnetism of the transition metal comes from the itinerant 3d electron band. The partially filled electron band which is filled up to the Fermi energy can be subdivided into two subbands with opposite spin orientation. The subbands are unequally occupied which leads to the raise of the magnetism in ferromagnet and when the external magnetic field is applied even in paramagnetic metal. The subbands are equally occupied in paramagnetic materials.

The 4f electrons of the *RE* are more localized and give the origin of the magnetic moment when the 4f electron shell is partially filed. The competition of the exchange interaction and the crystal field leads to a large diversity of magnetic structures. Very important is the interaction between the 3d and 4f electrons because the 3d-4f interaction couple the strongly anisotropic *RE* sublattice to the much less anisotropic T sublattice. This interaction is based on the indirect exchange interaction and is antiferromagnetic. With the Hund's rules, it explains ferromagnetic ordering when the *RE* is a lighter rare-earth and ferrimagnetic when *RE* is a heavier rare-earth.

It will be objective to derive the origin of the ferromagnetism in the Ising model. We have the system of spins placed on a lattice point and the interaction between the spins. The Hamiltonian of this system is defined as follows.

$$H = -\frac{1}{2}\sum_{mn} J_{mn} s_m s_n - \sum_m b_m s_m. \tag{2.8}$$

The indexes m, n indicate the lattice points, the variable s can swell two value $s_m \in \{+1, -1\}$ and means the direction of the spin (local moment) on the m-th lattice point.

The J_{mn} are the exchange integrals which describes the interaction of the spins ($J_{mm} = 0,\ J_{mn} = J_{nm}$). The b_m represents the local magnetic field (This coefficient will contain the external magnetic field). The Hamiltonian (2.8) is nonlinear. We have to make some approximation to find solution. The Hamiltonian without the perturbation:

$$H_0 = -\sum_m a_m s_m, \tag{2.9}$$

where the a_m represents the unknown local field. The Hamiltonian is in the "mean field" approximation and the a_m contain the effect of all the spins which can interact with the m-th spin.

The Hamiltonians H and H_0 is differ by the disturbance $V \equiv H - H_0$ and we can write the following inequality for the free energy F and F_0:

$$F \leq F_0 + \langle V \rangle_0 = F_0 + \langle H - H_0 \rangle_0 \,, \tag{2.10}$$

where $\langle \ldots \rangle_0$ means the thermodynamic mean value in respect with H_0. The quantity on the right side of (2.10) is equal to

$$F_0 = -\beta^{-1} \sum_m \ln \left[2 \cosh(\beta a_m) \right], \tag{2.11}$$

$$\langle H_0 \rangle_0 = -\sum_m a_m \langle s_m \rangle_0 \,, \tag{2.12}$$

$$\langle s_m \rangle_0 = \tanh \left(\beta a_m \right), \tag{2.13}$$

$$\langle H \rangle_0 = -\frac{1}{2} \sum_{mn} J_{mn} \langle s_m \rangle_0 \langle s_n \rangle_0 - \sum_m b_m \langle s_m \rangle_0 \,, \tag{2.14}$$

where $\beta = 1/k_B T$ and where we use the equation $\langle s_m s_n \rangle_0 = \langle s_m \rangle_0 \langle s_n \rangle_0$ which holds for noninteracting Hamiltonian H_0. Next step is to minimize the right side of (2.10). The condition of the minimum leads to the system of nonlinear equation.

$$a_j = b_j + \sum_n J_{jn} \tanh \left(\beta a_n \right), \qquad \langle s_j \rangle_0 = \tanh \left(\beta a_j \right) \tag{2.15}$$

The equation (2.15) can be interpreted this way: The mean value of the j-th spin s_j on the j-th lattice point is given by the value of the effective field a_j. The effective field is a sum of the applied field b_j and the term which contains the mean value of the spins on the others lattice points. The last term in equation (2.15) is spoken as the molecular Weiss field. The equation (2.15) represents the mean field approximation (MFA) from the Ising Hamiltonian (2.8).

If all the lattice points are equal we can write

$$b_m = b, \qquad a_m = a, \qquad \langle s_j \rangle_0 = \bar{s} \ \text{ and } \ \sum_n J_{mn} = J \tag{2.16}$$

and the equation (2.15) can be rewrite in form:

$$a = b + Js, \qquad \bar{s} = \tanh\left[\beta\left(b + J\bar{s}\right)\right] \tag{2.17}$$

The most of J_{mn} is positive in ferromagnet so the $J > 0$ and the (2.17) has nonzero solution for zero external field and temperature below the critical temperature T_c – the equation (2.17) leads to the arise of ferromagnetism. The hyperbolic tangent in (2.17) can be, form small field and high temperature, replace by $\tanh(x) \approx x$

$$\bar{s} = \frac{\beta b}{1 - \beta J} = \frac{b}{k_B T - J} \tag{2.18}$$

and write in usual form as Currie-Weiss law

$$\bar{s} = \chi b, \qquad \chi(T) = \frac{1}{k_B T - J} \tag{2.19}$$

The MFA has some objection as for example wrong critical exponents and very slow fall of the magnetization from the saturated value at the low temperature.

2.2 Basic concept of the magnetocaloric effect

For simple concept we can imagine that there are microscopic magnetic moments in the material. The microscopic magnetic moments are influenced by the random thermal motions at any finite temperature. When applying the magnetic field the microscopic moments are forced to aligned to the magnetic field direction and the energy of the moments is changed. The energy of the lattice is then changed via the spin-lattice coupling and we can observe the adiabatic temperature change.

The temperature dependence of the entropy for the para- or ferromagnetic material is shown in figure 2.1. The arrows in the figure 2.1 represents the adiabatic temperature change ΔT and the isothermal entropy change ΔS, respectively. In case of a material in a paramagnetic or a ferromagnetic state the isothermal change of entropy is negative and the adiabatic temperature change is positive when applying the field. The isothermal change of entropy is positive and the adiabatic temperature change is negative when the material is in an antiferromagnetic state. The magnetocaloric effect reaches maximum when the ordering of the magnetic moments changes very rapidly with a small change of the magnetic field. Such case represents the phase transition.

There are two type of the phase transitions in the nature. We speak about first order transition if there is a jump in the first derivative of the Gibbs free energy. The second order transition is characterized by the continuous first derivative and discontinuous second derivative of the Gibbs free energy. The Gibbs free energy is generally given by following

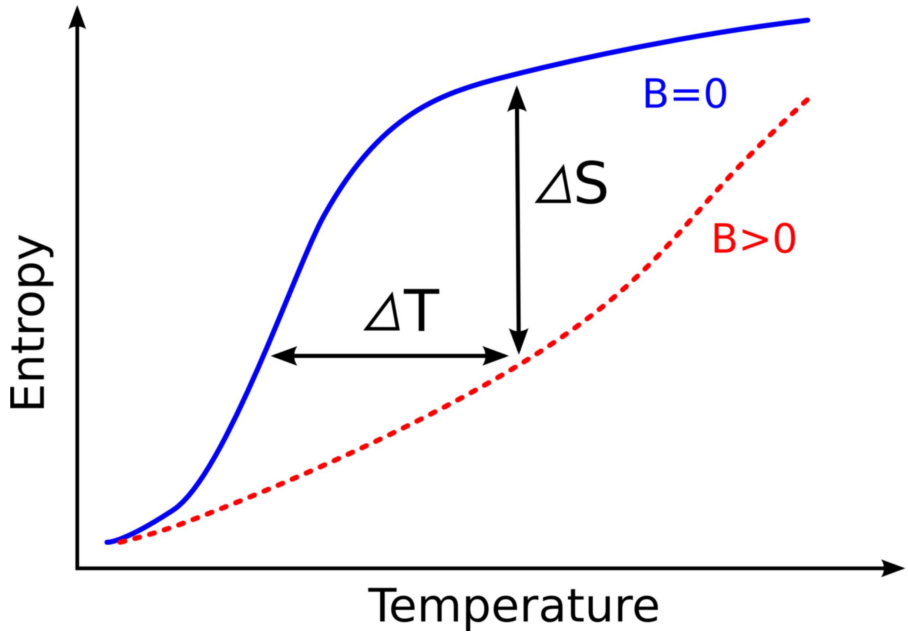

Figure 2.1: The illustrative evolution of the entropy with applied magnetic field and without the field. The arrows represent the adiabatic temperature change and the isothermal entropy change. The dependence corresponds to a ferromagnet or a parramagnet.

equation:

$$G = U - TS + pV - MB, \tag{2.20}$$

where the U is internal energy, T is temperature, S is entropy, p is pressure, V is volume, M is magnetization and B represents the magnetic field. Although the temperature dependence of the entropy change, ΔS, reaches very high value when the first order transition occurs, the width of the maximum is very small. The volume change and the hysteresis of the magnetocaloric effect at the first order transition poses is a great obstructions for the real application. The second order transition brings broader maximum of the entropy change and the absolute value of this maximum is only fraction of values measured at the first order transition. There is no hysteresis at the second order transitions.

The knowledge of the fundamental thermodynamic relations is important to proper understanding of the magnetocaloric effect. Entropy S, magnetization M and volume V can be expressed as the first derivative of the Gibbs free energy (2.20) and the following equation can be written:

$$S(T, B, p) = -\left(\frac{\partial G}{\partial T}\right)_{p,B}, \tag{2.21}$$

$$M(T, B, p) = -\left(\frac{\partial G}{\partial B}\right)_{T,p}, \tag{2.22}$$

$$V(T, B, p) = \left(\frac{\partial G}{\partial p}\right)_{T,B}. \tag{2.23}$$

It is possible to write the entropy differential:

$$dS = \left(\frac{\partial S}{\partial T}\right)_{p,B} dT + \left(\frac{\partial S}{\partial p}\right)_{T,B} dp + \left(\frac{\partial S}{\partial B}\right)_{T,p} dB. \tag{2.24}$$

The first two parts of the sum in (2.24) can be expressed as:

$$\left(\frac{\partial S}{\partial T}\right)_{p,B} dT = \frac{c_{B,p}}{T} dT, \qquad \left(\frac{\partial S}{\partial p}\right)_{T,B} dp = -\alpha V dp, \tag{2.25}$$

where $c_{B,p}$ is the heat capacity in constant magnetic induction and constant pressure and α is the coefficient of the thermal expansion. The equation (2.24) for the adiabatic-isobaric process ($dS = 0$, $dp = 0$) takes the following form:

$$\left(\frac{\partial S}{\partial B}\right)_{T,p} dB = \frac{c_{B,p}}{T} dT. \tag{2.26}$$

The magnetization isotherms or the heat capacity measurement are very often used to enumerate the magnetocaloric effect. We need the Maxwell relation

$$\left(\frac{\partial S(T,B)}{\partial B}\right)_{T,p} = \left(\frac{\partial M(T,B)}{\partial T}\right)_{B,p} \tag{2.27}$$

and definition of the heat capacity

$$c_p = T\left(\frac{\partial S}{\partial T}\right)_p \tag{2.28}$$

for such calculation. The Maxwell relation express the mathematical fact that the first derivatives of the Gibbs free energy can be switched if they are smooth. This means that the Maxwell relation can be used only in system which undergo the second order transition but not in systems with the first order transition. The Maxwell relation is still used in case of the first order transition as a rough estimation.

The equation (2.27) can be integrated and the final relations to calculate the ΔS_m from the magnetization isotherms is obtained (considering field change from 0 to B_1):

$$\Delta S_m = \int_0^{B_1} \left(\frac{\partial M(T,B)}{\partial T}\right)_B dB. \tag{2.29}$$

The integration of (2.28) gives

$$S = S_0 + \int_0^T \left(\frac{c_p(T',B)}{T'}\right) dT', \tag{2.30}$$

where S_0 is field independent. If we know the heat capacity in two different magnetic

fields, we can calculate the entropy change according to following equation:

$$\Delta S_m = \int_0^T \left(\frac{c_p(T', B_0) - c_p(T', B_1)}{T'} \right) dT'. \tag{2.31}$$

The magnetization and heat capacity measurements are not continues, so we have to enumerate the integral and the derivative using some numerical method. We have to enumerate the area below the integrated curve in principle. In our work we use the rectangular method of integral enumeration. The equations (2.29) and (2.31) can be than written as follows:

$$\Delta S_M(T_{av}, H_N) = \sum_{l=1}^{N-1} \frac{M(T_{i+1}, H_l) - M(T_i, H_l)}{T_{i+1} - T_i} \ (H_{l+1} - H_l), \tag{2.32}$$

$$\Delta S_M(T_N, H_1) = \sum_{l=1}^{N-1} \frac{c(T_l, H_0) - c(T_l, H_1)}{T_l} \left(T_{l+1} - T_l\right), \tag{2.33}$$

where T_{av} is the average of the temperatures T_i and T_{i+1}. Another numerical method is the trapezoidal method. The trapezoidal method use the trapezoids in place of rectangular to approximate the area below the integrated curve. The difference is for large N negligible and both methods give the same results.

Another quantity to compare the different magnetocaloric materials is the relative cooling power (RCP). The RCP represents the mass of heat which can be transfered in one cooling circle and is important for the real application. The RCP is product of the maximum entropy change (ΔS_m^{max}) and the full width at half of the maximum of the temperature dependence of the entropy change (δT_{FWHM}):

$$RCP = \Delta S_m^{max} * \delta T_{FWHM}. \tag{2.34}$$

2.3 Influence of substitutions

The change of the chemical composition is one of the way how to alter the material properties to be, for example, suitable for application (the properties of steel or the transition temperature of the magnetocaloric materials) but also to alter the position of the interesting physical phenomena to be in experimentally reachable area. The substitution takes place as a so called tuning parameter when studying the quantum critical phenomena, too. In general, the substitution can lead to a change of the electron density of states (DOS) and also leads to a change of crystallographic parameters or even can lead to a change of the crystal-structure type. Both modifications, electronic and crystallographic, influence the magnetic ordering. In some cases (when the substitution is very close to the substituted atoms) are the effects of substitution compared with the pressure effect. The

pressure can change the lattice parameter of the system but do not change the chemical composition.

The substitution in this work was used mainly to change the ordering temperature. In this way, we can tune the maximum of MCE to the desired temperature region. Within the frames of this work, it is the case of $RE\mathrm{Co}_2$ system and Gd-Tb alloys. The size of MCE can also vary dramatically upon substitution due to various reasons like a change of the magnetic moment size or (dis)appearance of crystallographic changes. We will show that substitutions studied in this work do not lead to any prominent changes of the size of MCE.

Chapter 3

Experimental methods

3.1 Sample preparation

Polycrystalline samples were prepared by arc-melting from the stoichiometric melt of pure metals. The purity of metals were 3N for Dy, Gd, Tb and Co, 3N5 for Rh and 3N8 for Fe. The melting was done in the mono-arc furnace in an argon atmosphere. The pure elements were put in the water cooled copper boat and melt several times to ensure the homogeneity. The boat was spherical in case of $RECo_2$ compound. The Gd-Tb alloys were first melted in the spherical boat than cracked in the pieces and finally remelted in an rectangular boat with cross-section 5×5 mm. The length of the prepared samples was about 20 or 30 mm. The rectangular shape is more suitable for subsequent rolling.

$RECo_2$ samples were then annealed for one week at temperatures of 950 °C for $DyCo_2$ series and 925 °C for $GdCo_2$ series. Three samples of $Dy(Co_{1-x}Fe_x)_2$ with x = 0.00, 0.01 and 0.03 were prepared. Six samples of $Gd(Co_{1-x}Rh_x)_2$ with x = 0.05 up to 0.30 were prepared.

Six samples of Gd-Tb alloys were prepared with Tb concentration of 0, 10, 20, 25, 30 and 40%. The sample with 10% of Tb was also rolled into very thin (∼0.03 mm) ribbon. After then the samples of different shape were made from this ribbon to investigate the influence of sample shape on the magnetocaloric effect.

The DyNiAl single crystal was grown by Czochralski method in a tri-arc furnace from the stoichiometric melt of the constituent elements as described in detail in [25]. The nearly cubic piece of 1.6 mm^3 cut from the crystal used also in the previous studies [25–27] was used in the present work.

3.2 Sample characterization

The prepared samples were characterized by the x-ray diffraction to determine the phase purity, structure and structural parameters. The powder diffraction was performed on

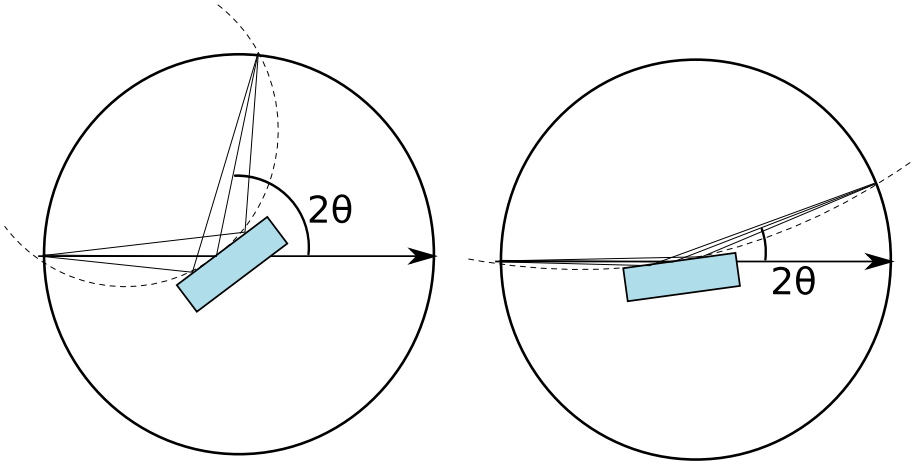

Figure 3.1: The Bragg-Brentano geometry. The punctuated circle is the focus circle, the full circle is the detector circle.

the diffractometers with Bragg-Brentano geometry. The arrangement can be seen on the figure 3.1. The sample is in the central axes and sample face is tangential to the focus circle. The detector of the diffracted beam is free to go along the circle around the sample with twofold angle velocity then the sample velocity. The positions of the maxima of diffracted intensity are given by the Bragg law:

$$2d_{hkl} \sin\theta = \lambda, \tag{3.1}$$

where d_{hkl} is the distance between crystal planes, θ is the angle of the diffracted wave (as can be seen in 3.1) and λ is the x-ray wavelength. The x-ray analysis of the samples was performed on two diffractometers: Brucker and Siemens (installed at the Department of Electronic Structures at the Charles University). The radiation of Cu with the wavelengths $\lambda(K_{\alpha 1}) = 1.5405 \times 10^{-10}$ m and $\lambda(K_{\alpha 2}) = 1.5445 \times 10^{-10}$ m was used for the experiment. The diffractogram was evaluated by using the FullProf software [28]. The lattice parameters were refined from the peak positions. Several extrinsic peaks found in $RE\mathrm{Co}_2$ samples indicate the presence of a small amount of impurity phases.

3.3 Measurement of the magnetocaloric effect

3.3.1 Indirect methods

Two methods are used to determine the magnetocaloric effect indirectly in this work. First we studied the magnetic isotherms at different temperatures $M_T(H)$. Measurement was done on the commercial instrument MPMS provided by Quantum Design. The entropy change can by calculated from knowledge of the magnetic isotherms according to equation (2.32). The samples of $RE\mathrm{Co}_2$ were measured in plastic capsule as fixed powder. The

samples of Gd-Tb alloys can not be pulverized so the measurements were performed on the small elliptical chips. In case of $Gd_{0.9}Tb_{0.1}$ sample, special shapes as described in the next chapter were used. The error of this method is about 20% and can be calculated according the following equation:

$$\eta_{\Delta S} = \sum_{k=1}^{N-1} \left(\eta_M \frac{M_k^{T_1} + M_k^{T_2}}{M_k^{T_2} - M_k^{T_1}} + \eta_H \frac{H_{k+1} + H_k}{H_{k+1} - H_k} \right) + \eta_T \frac{T_1 + T_2}{T_2 - T_1}. \tag{3.2}$$

Here η is the relative error of the quantity in the subscript and $\frac{T_1+T_2}{2}$ is the T_{av}. The subtraction of two close values of magnetization and the subsequent sum of this difference is the main source of the error.

The heat capacity was measured in several different magnetic fields $c_H(T)$. These measurements were performed on the commercial instrument PPMS provided by Quantum Design. The heat capacity can tell us not only the isothermal entropy change (equation (2.33)) but also the adiabatic temperature change of the material. Absence of an easy way how to fix the samples which have a large value of the magnetic moment is a great problem of this measurement.

3.3.2 Direct measurement

The third method used in this work is the direct measurement of the temperature change when applying the magnetic field. This measurement was performed on the unique instrument design by Ing. Kamarád. The device can operate in the temperature range from 330 K to 80 K. The liquid nitrogen is used as a cooler and the heating wire is used as a heater. Magnetic field is produced by the Halbach magnet and can reach 1 T. Cryostat is free to go in and out the field and it is possible to rotate the cryostat, too. The temperature of the sample is registered during the process of relaxation of the sample after moving in or out of the magnetic field. The temperature is measured by two thermocouples. One can extrapolate the temperature change ΔT of the sample from measured relaxation.

When using this method, we face several problems. The firs and the most severe one is the thermal contact between the thermocouple, the sample and the sample holder. The sample gives the heat to the thermocouple and in the same time to the sample holder when we change the sample temperature by changing the field. The relaxation can be distort if the relaxation process is too fast and the subsequent interpolation has larger error. The large samples partially solve this problem by enhancement of the relaxation time.

The next problem is connected with the changing of the field. Since the movement of the cryostat is performed by hand, the alternation of the magnetic field is not exactly the same at all measurements. The recorded data has to be erased if there were disturbances in the fluent movement. The measurement is performed several times and the mean value

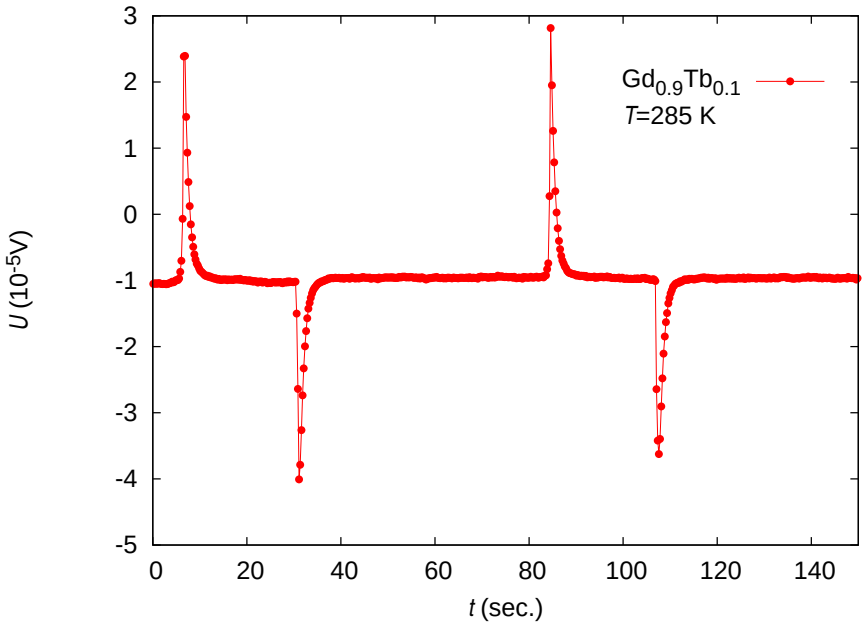

Figure 3.2: The time dependence of the voltage on the thermocouples. The voltage corresponds to the temperature difference between the sample and the sample holder. The data were obtained on the $Gd_{0.9}Tb_{0.1}$ at 285 K and the peaks correspond to the field change of 1 T.

is calculated.

The recorded data for the sample $Gd_{0.9}Tb_{0.1}$ measured at 285 K can be seen in figure 3.2. The voltage U on the y-axis corresponds to the difference between the sample temperature and the sample holder temperature according to the relation

$$\Delta T[K] = \frac{U[V]}{4.10^{-5}[V.K^{-1}]}. \tag{3.3}$$

The peaks represent the moving in or out the magnetic field. First the time dependence of the "background" temperature difference (the difference between the sample temperature and the sample holder temperature when the field is constant) is extrapolated by the linear dependence. The recorded data of each movement are then extrapolated by the Newtons law of cooling:

$$T(t) = T_0 + \Delta T_{max} * \exp\left(\frac{-t}{\tau}\right), \tag{3.4}$$

where T_0 is starting temperature of the sample, ΔT_{max} is the temperature change, t is time and τ is constant which contains the heat capacity of the sample, sample weight and thermal transfer coefficients.

Chapter 4

Results and discussion

4.1 Anisotropic magnetocaloric effect in DyNiAl

This compound crystallizes in the hexagonal ZrNiAl-type structure, orders magnetically below $T_C = 31$ K and undergoes a further magnetic phase transition at $T_1 = 15$ K. The Dy-moments are aligned ferromagnetically along the hexagonal c-axis below T_C, the additional antiferromagnetic component develops within the basal plane below T_1 [27].

In order to determine the anisotropy of the magnetocaloric effect in DyNiAl, we have measured in detail the magnetization curves with magnetic field applied along the hexagonal c-axis and perpendicular to the c-axis. In the second orientation, the field was oriented along the a-axis, but considering the previous studies [26, 27], possible anisotropy of MCE within the basal plane is rather small.

The magnetization curves are represented in figure 4.1 for magnetic field oriented along the c- and a-axis, respectively.

The measurements were performed between 2 and 40 K with a 2 K step, additional $M(H)$ dependence was measured for $H \parallel a$ at 50 K. The results are well in agreement with the previously measured data [25]. We observe a typical ferromagnetic behavior for magnetic field parallel to the hexagonal c-axis. When applying magnetic field along the a-axis, we observe a low initial susceptibility reflecting the strong uniaxial anisotropy. Field-induced transition is observed between 1.5 and 2 T, both below and above T_1. We can exclude its metamagnetic nature because above T_1 the compound is a simple collinear uniaxial ferromagnet. Therefore, we can consider this transition as a rotation of the ferromagnetic component of the dysprosium magnetic moment from the c-axis to the basal plane. This interpretation is corroborated also by the neutron-diffraction results [27]. The resulting magnetic structure is stable in a wide interval of further increasing field, the additional transition occurs only in high fields around 12 T [25].

The magnetic entropy change, $-\Delta S_m$, was derived from the $M(H)$ dependencies using the equation (2.32). The results are displayed in figures 4.2 and 4.3. We note that

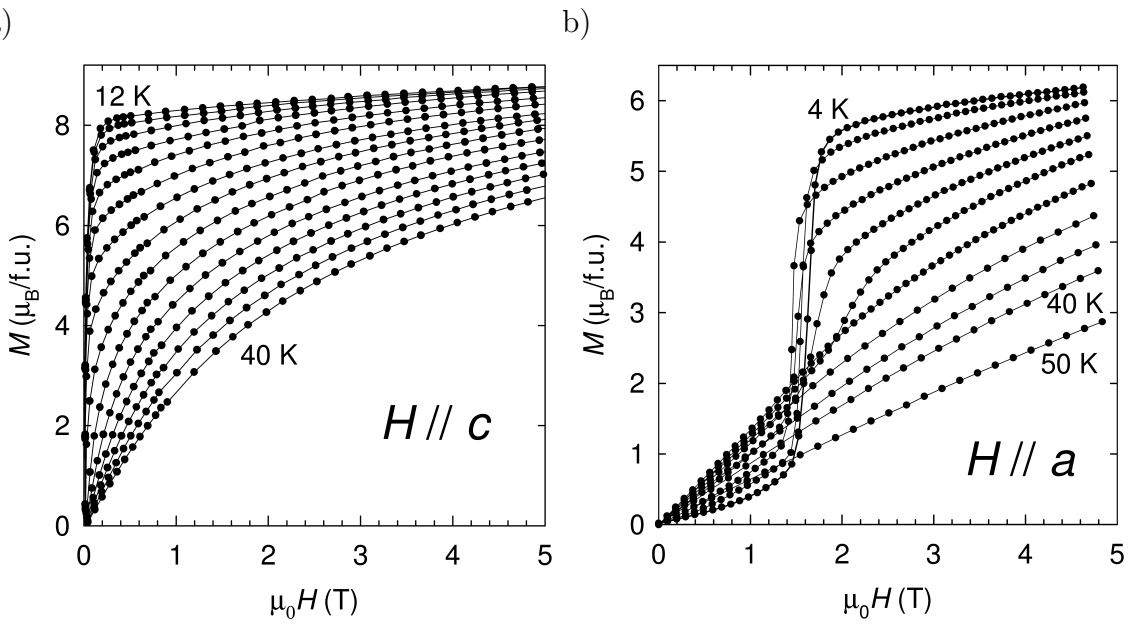

Figure 4.1: The magnetization curves of DyNiAl a) measured with field applied along the c-axis. The curves between 12 K and 40 K are shown with the step of 2 K; the curves measured below 12 K are not displayed because they almost overlap with that obtained at 12 K. b) measured with field applied along the a-axis. The curves between 4 K and 40 K are shown with the step of 4 K, i.e. only every second curve is shown for better lucidity.

1 J.K^{-1}.kg^{-1}=0.248 J.K^{-1}.mol^{-1}.

When the field is applied along the c-axis, the entropy change shows a maximum near the ordering temperature T_C and reaches the value of $-\Delta S_m = 14$ and 22 Jkg^{-1}K^{-1} for 2 and 5 T, respectively. This behavior clearly reflects the ferromagnetic ordering of Dy moments along the c-axis. For the perpendicular orientation, $H \parallel a$, the behavior is much more complex. We observe a small negative MCE (positive ΔS_M) for the applied field of 1 T what reflects the antiferromagnetic character of the magnetic order within the basal plane below T_1 [27]. The negative MCE persists also between T_1 and T_C, indicating the antiferromagnetic type of interactions in this temperature region. The entropy change related to the antiferromagnetic component increases with increasing magnetic field, leading to the total value of 2 Jkg^{-1}K^{-1} below 10 K in 2 T. The antiferromagnetic order remains intact also in higher fields and certainly contributes to the entropy change, but the total MCE is strongly influenced by the field-induced transition in ≈ 1.5 T related to the rotation of the ferromagnetic component from the c-axis to the basal plane. The total entropy change gradually becomes negative and we observe two moderate maxima of $-\Delta S_m$: around the T_C and around 19 K. The existence of a minimum around 24 K is related to the fact that the field-induced transition shifts to higher fields for temperatures above 20 K (see figure 4.1). The size of the entropy change for $H \parallel a$ and $H \parallel c$ is well comparable below T_1, but the maximum in $-\Delta S_m$ around T_C for $H \parallel c$ is considerably larger than any values for the perpendicular orientation.

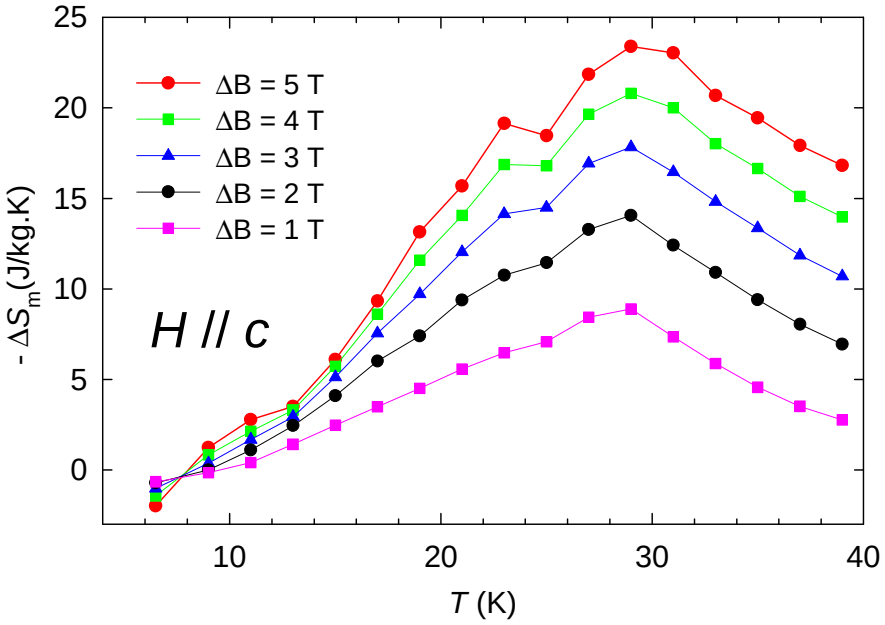

Figure 4.2: The magnetocaloric effect in DyNiAl as determined from the magnetization curves with magnetic field applied along the c-axis. We note that 1 J.K^{-1}.kg^{-1}=0.248 J.K^{-1}.mol^{-1}.

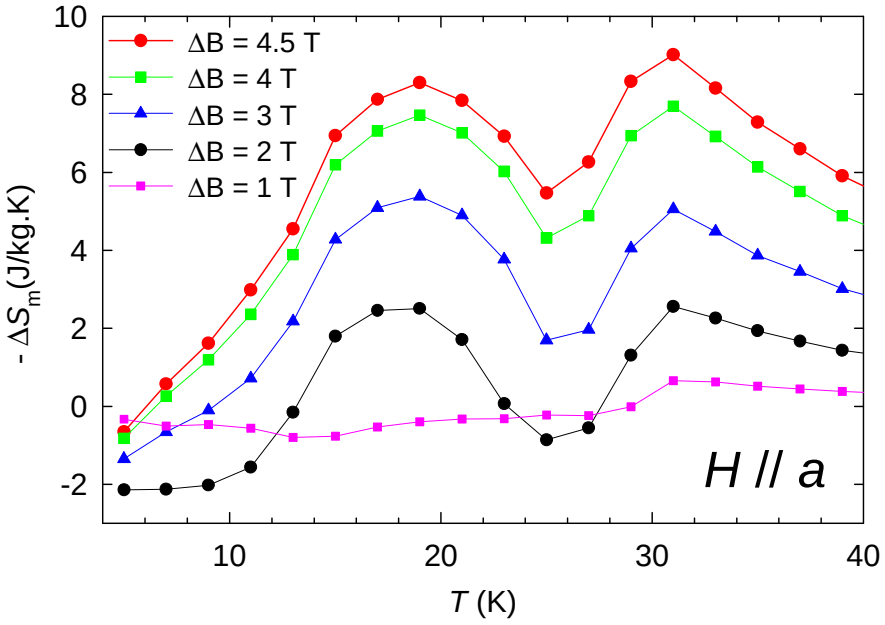

Figure 4.3: The magnetocaloric effect in DyNiAl as determined from the magnetization curves with magnetic field applied along the a-axis. We note that 1 J.K^{-1}.kg^{-1}=0.248 J.K^{-1}.mol^{-1}.

The existence of two or even more maxima in the entropy change is often observed in compounds exhibiting multiple phase transitions, e.g. Tb_5Ge_4 [29]. The case of DyNiAl and $H \parallel a$ is different, although also DyNiAl undergoes two magnetic phase transitions. The observation of the two maxima in $-\Delta S_m$ is related here to the nature and temperature development of the field-induced transition and occur only if the applied field exceeds the value of this transition (see figure4.3).

Our results reveal a strong anisotropy of the MCE in DyNiAl. We observe a large entropy change for magnetic field parallel to the easy magnetization c-axis whereas ΔS_m is smaller and has a very complex temperature dependence for the perpendicular orientation $H \parallel a$. The results obtained for $H \parallel c$ are qualitatively similar to those reported on polycrystalline sample [15], but the size of the MCE is considerably enhanced. The value of $-\Delta S_m = 14$ Jkg^{-1}K^{-1} obtained in our study for the field of 2 T represents $\sim 40\%$ increase compared to the value of 10 Jkg^{-1}K^{-1} obtained on polycrystal for the same field. The polycrystalline data represent some average of all the crystallographic directions, so the grains oriented with the c-axis perpendicular to the applied field lessen the total MCE.

Another quantity characterizing MCE is the adiabatic temperature change ΔT_{ad}. Its temperature dependence calculated from the entropy change with the field applied along the c-axis and the specific heat data (see figure 4.4) is shown in figure 4.5. The maximum position in $\Delta T_{ad}(T)$ is shifted to higher temperatures when compared to the $-\Delta S_m(T)$ dependence because the temperature change strongly depends also on the slope of the entropy curve $S(T)$ (see inset of figure 4.4). The same entropy change results in a larger temperature change when the slope of the $S(T)$ curve is smaller. The maximum values of ΔT_{ad} are found to be 4.5 and 7.8 K, for field changes of 2 and 5 T, respectively. The value obtained for the 2 T change represents about 30 % increase compared to the $\Delta T_{ad} = 3.5$ K found in polycrystalline sample [15].

The relative cooling power, RCP, is also used when comparing different magnetocaloric materials. We can roughly estimate the RCP values of DyNiAl with field applied along c-axis to be 280 and 600 Jkg^{-1} for the 2 and 5 T change, respectively.

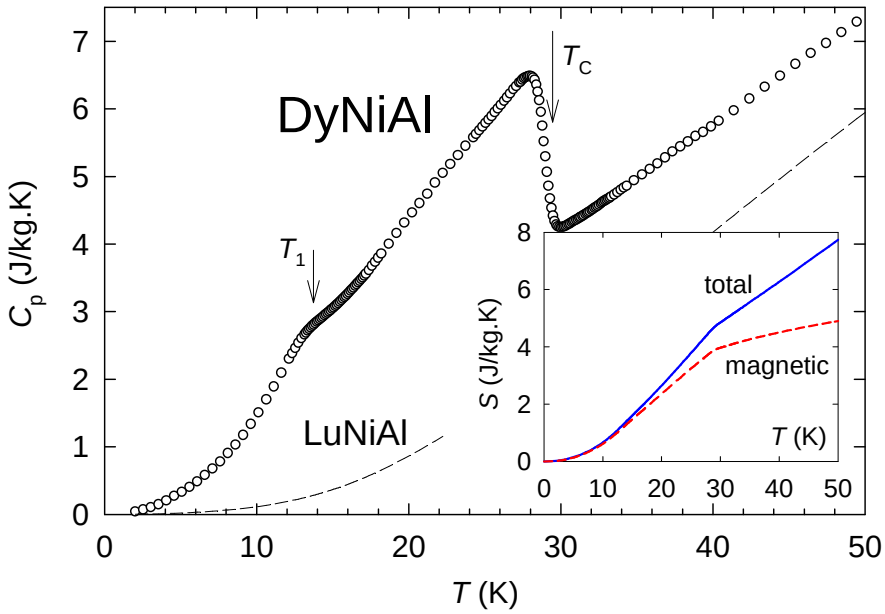

Figure 4.4: The specific heat of DyNiAl, data taken from Ref.[26]. Inset shows the total (full blue line) and magnetic (dashed red line) entropy estimated using the LuNiAl data as a nonmagnetic analogue.

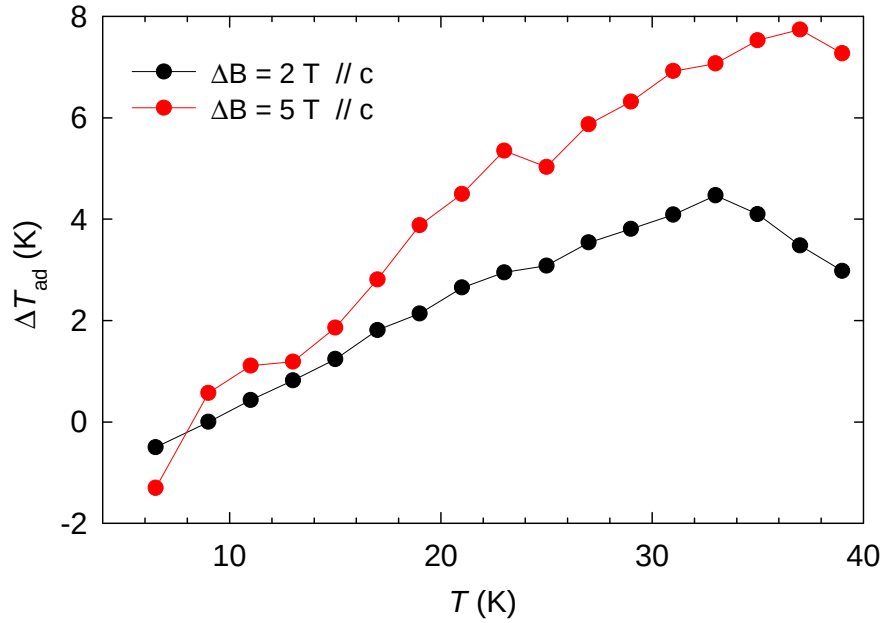

Figure 4.5: The adiabatic temperature change in DyNiAl calculated form the entropy change and the specific heat data (see figure 4.4) for magnetic field applied along the *c*-axis.

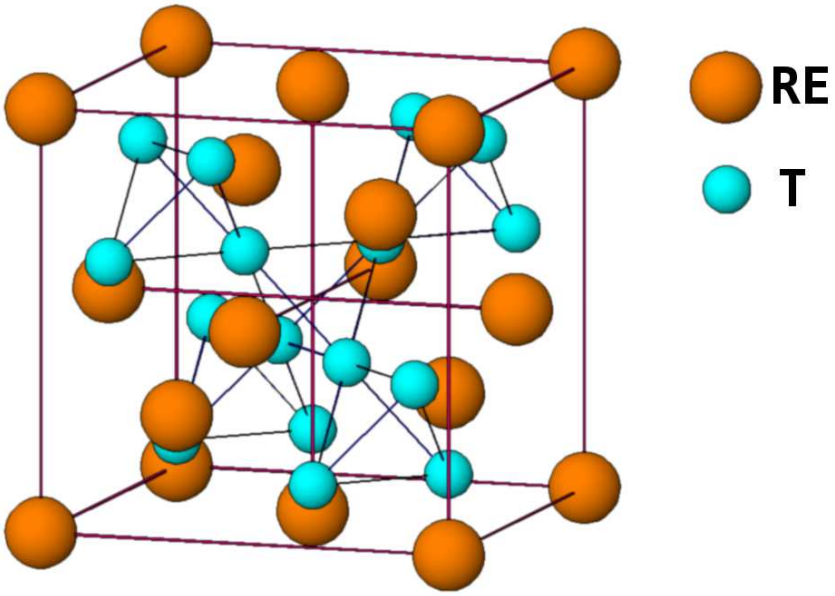

Figure 4.6: The unit cell of the RE-T_2 compounds. RE represents the rare-earth metal (Gd, Dy) and T stands as transition metal (Fe, Co, Rh).

4.2 Substituted $RECo_2$

The intermetallic RCo_2 compounds belong to some promising materials showing considerable magnetocaloric effect. In RCo_2 containing a magnetic rare earths, a Co magnetic moment is induced by the internal field due to the ordered rare-earth moments. For heavy-rare-earth compounds an antiparallel coupling of rare-earth and cobalt moments is evidenced. The magnetic phase transitions are of first order for RE = Er, Ho or Dy, and of second order for the other rare-earth atoms (see e.g. Gratz and Markosyan [30]).

We present the influence of substitutions on magnetocaloric effect in two systems. The first system is $Gd(Co_{1-x}Rh_x)_2$ and the second system is $Dy(Co_{1-x}Fe_x)_2$. These systems crystallize in the cubic C-15 Laves phase $MgCu_2$-type structure. The structure is figured in 4.6. $GdCo_2$ shows the second-order magnetic phase transition near 400 K [31], $DyCo_2$ undergoes the first-order transition at 142 K [32]. There is the antiferromagnetic interaction between the rare-earth sublattice and the transition metal sublattice because the Dy and the Gd belongs to the heavy rare-earth. The Rh substitution in $Gd(Co_{1-x}Rh_x)_2$ should decrease the transition temperature, whereas the Fe substitution will increase the ordering temperature in $Dy(Co_{1-x}Fe_x)_2$. We tune both systems to exhibit substantial magnetocaloric effect in the range between 200 and 300 K.

Although magnetocaloric effect in the $Dy(Co_{1-x}Fe_x)_2$ has been already studied by Han et al. [33], we believe that it is interesting to compare both presented systems within one work, i.e with the same way of sample preparation and measurement. We also present different Fe concentrations than Han et al.[33].

4.2.1 Gd(Rh,Co)$_2$

In this work we try to tune the transition temperature to range between the 200 and 300 K by changing the Rh concentration in the Gd(Rh$_{1-x}$Co$_x$)$_2$ with x between 0.05 and 0.30. The x-ray powder diffraction was performed on prepared samples. The concentration dependence of the lattice parameter (figure 4.7) was found out from diffraction patterns. The lattice parameter in Gd(Rh,Co)$_2$ increases almost linearly with the Rh concentration as can be assumed taking into account the atomic volumes of Co and Rh.

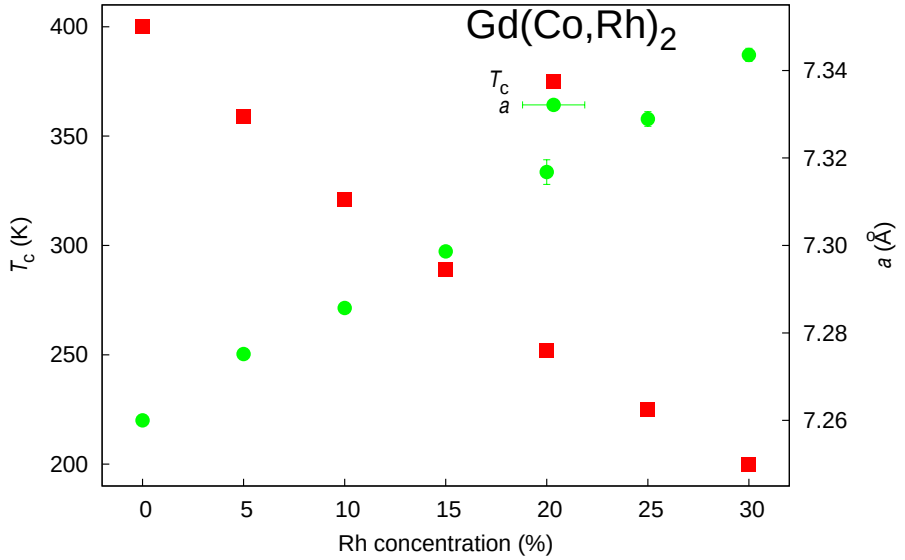

Figure 4.7: The concentration dependence of the transition temperature T_c and the lattice parameter a. The value of $a = 7.26$Å and $T_c = 400$ K for pure $GdCo_2$ is taken from [31].

The magnetic measurement was done in order to obtain the transition temperature and to determine the magnetocaloric effect. The temperature dependence of the magnetization in a very small magnetic field (∼0.01 T) was measured for each sample. Measured curves are plotted in figure 4.8. The magnetization was measured when cooling the samples. The transition temperature was obtained as the temperature at which the first derivative of the magnetization with respect to the temperature has a maximum. The errors of transition temperatures are about 2 K and depend on the steepness of the temperature dependence of the magnetization. The concentration dependence of T_c plotted in figure 4.7 shows significant, linear decrease with increasing the Rh content. The value of T_c and lattice parameter for pure $GdCo_2$ taken from [31] fit very well the linear character of the concentration dependence found in our study. The influence of Rh substitution can be compared with the Mn substitution [34]. However the dependence is more complicated in the Mn case – the decrease of the transition temperature at higher Mn concentration is preceded with the increasing of T_c at low concentration.

The quarter of magnetization isotherm was measured in a wide temperature range

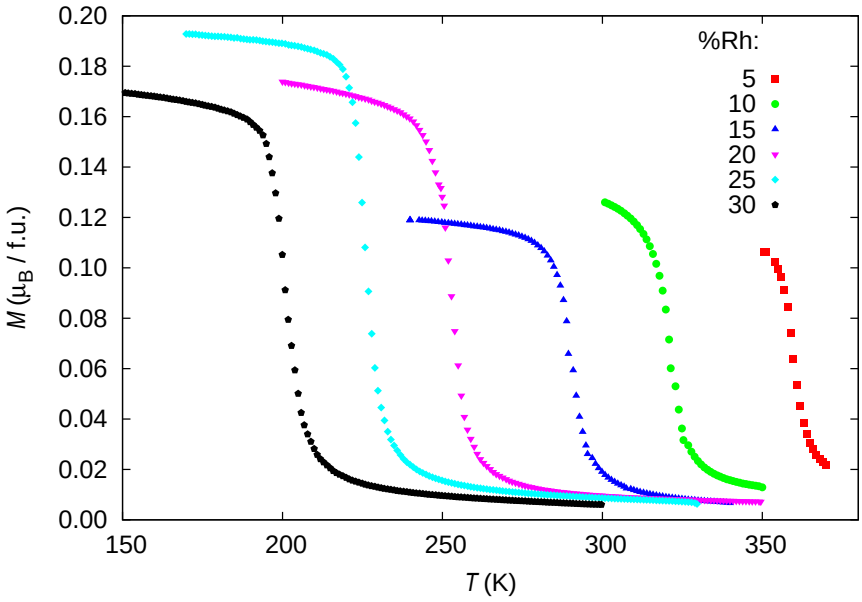

Figure 4.8: Temperature dependence of magnetization in $Gd(Co,Rh)_2$ system measured in a field of ∼0.01 T.

around T_c for samples with Rh concentration higher then 5%. The $Gd(Rh_{0.05}Co_{0.95})_2$ sample has $T_c = 359\ K$ which is too high to perform the measurement around T_c. Representative example of the magnetization isotherms is shown in figure 4.9. The isotherms were measured with 4 K step and 2 K step nearby the transition temperature and the magnetic field was altered from 0 up to 5 T.

The entropy change ΔS_m was calculated according to equation (2.32) and is represented in figure 4.10 for the field change of 1 and 5 T. The maximum of the negative entropy change $-\Delta S_m^{max}$ slightly increases when the T_c decreases and swell the value between 0.86 and 1.11 $Jkg^{-1}K^{-1}$ for the field change of 1 T and 3.05 and 3.86 $Jkg^{-1}K^{-1}$ for the field change of 5 T. The representative error calculated according to equation (3.2) is represented in figure 4.10 by the error bars for two concentrations (10% and 30% of Rh). The width of the temperature dependence of ΔS is important for the application so that the RCP value is calculated according to (2.34). All obtained values are summarized in table 4.1.

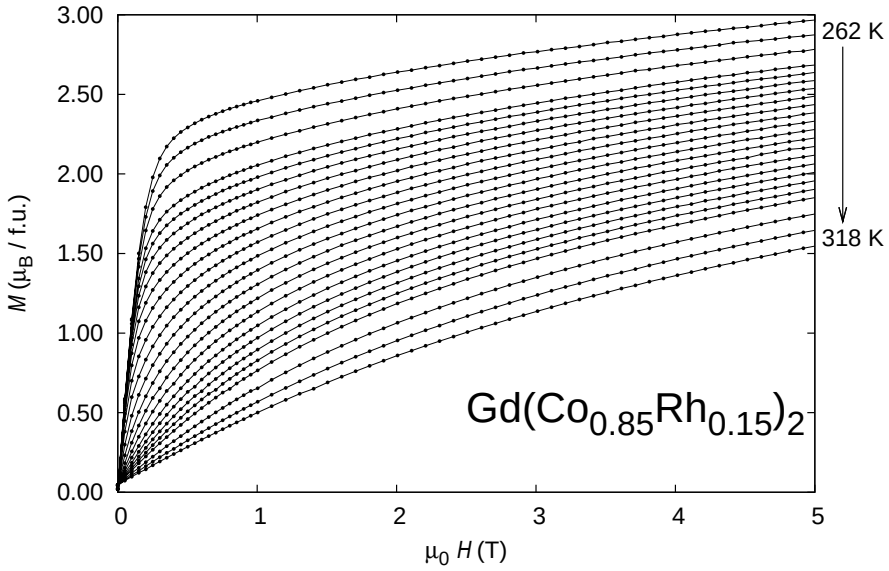

Figure 4.9: Magnetization isotherms of the $Gd(Co_{0.85}Rh_{0.15})_2$ measured at different temperatures around $T_c = 289$ K. The data were measured with a 2 K steps in vicinity of the transition and with 4 K step far from the transition.

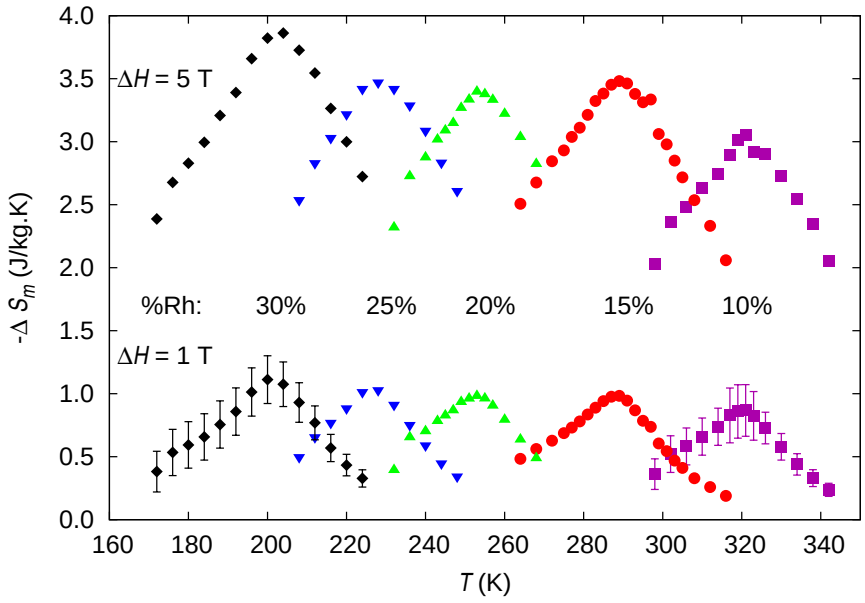

Figure 4.10: The entropy change for the $Gd(Co_{1-x}Rh_x)_2$ system for the magnetic field change from 0 to 1 T and from 0 to 5 T. The estimated errors are presented for concentration of 10% and 30% of Rh. We note that 1 $J.K^{-1}.kg^{-1} \doteq (0.216 + 0.044x)$ $J.K^{-1}.mol^{-1}$.

Table 4.1: The structural and magnetocaloric characteristics of the $Gd(Co_{1-x}Rh_x)_2$ series. We note that 1 $J.K^{-1}.kg^{-1} \doteq (0.216 + 0.044x)$ $J.K^{-1}.mol^{-1}$ (* valid for the field change from 0 to 1 T; ** valid for the field change from 0 to 5 T)

x	a (Å)	T_c (K)	-ΔS (J/K.kg) *	-ΔS (J/K.kg) **	RCP (J/kg)
0.05	7.275	359	-	-	-
0.10	7.285	321	0.87	3.05	30
0.15	7.298	289	0.98	3.48	36
0.20	7.316	252	0.98	3.40	36
0.25	7.328	225	1.03	3.47	36
0.30	7.343	200	1.11	3.86	42

4.2.2 $Dy(Fe,Co)_2$

We prepared three samples of the $Dy(Fe_{1-x}Co_x)_2$ with x=0.00, 0.01, 0.03. The x-ray powder diffraction was performed in order to obtained the lattice parameter. The concentration dependence of the lattice parameter is shown in figure 4.11. The lattice parameter is almost unchanged as expected. The error of the lattice parameter is given by the FullProf software.

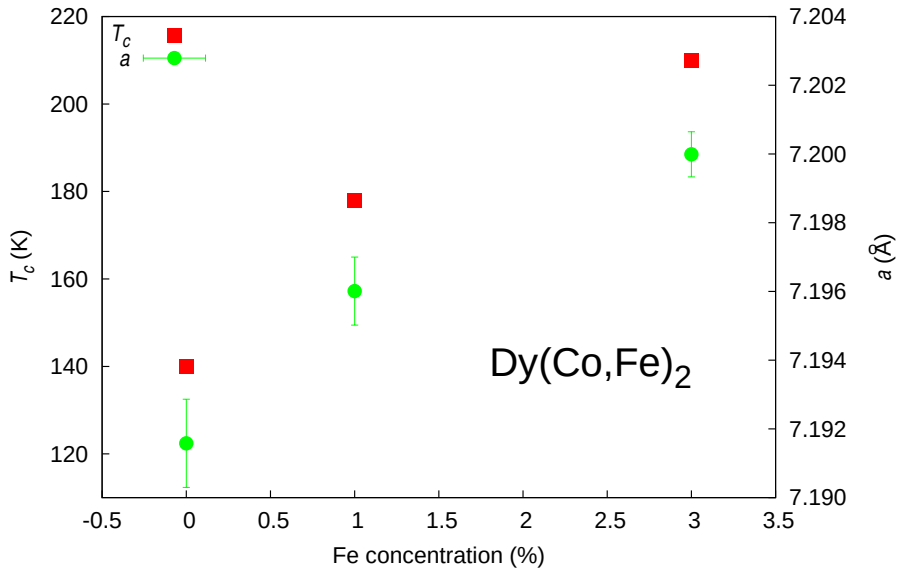

Figure 4.11: Concentration dependence of the lattice parameter (right scale) and ordering temperature (left scale) of the $Dy(Co,Fe)_2$ system.

The temperature dependence of the magnetization, represented in figure 4.12, was measured on all prepared samples in small magnetic field (∼0.01 T) to determine the transition temperature. The transition temperature was obtained as the maximum of the first derivative of the magnetization with respect to the temperature. The error of determination of transition temperatures is about 2 K. The concentration dependence of the transition temperature is in figure 4.11. The small amount of iron addition leads

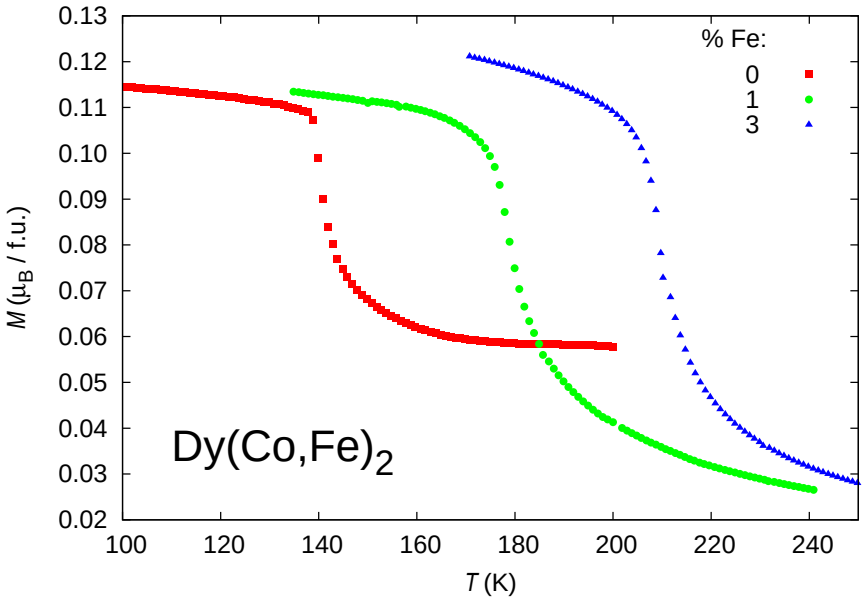

Figure 4.12: Temperature dependence of magnetization in $Dy(Co,Fe)_2$ system measured in a field of ∼0.01 T.

to the huge enhancement of the transition temperature. The change of the sharp curve shape for the pure $DyCo_2$ to the smooth curve shape for the doped samples suggest the change of the phase transition from the first-order for the pure $DyCo_2$ compound to the second-order transition for the doped samples.

The field dependence of the magnetization was measured in a wide temperature range. The field was altered up to 5 T but only up to 1 T the data can be used and for the sample with 0% of iron even less. The higher magnetic field caused the release of the sample probably due to the large anisotropy of dysprosium and/or insufficient fixing of the powder. The example of measured magnetization is in figure 4.13. The magnetization isotherms were measured with a 2 K step. The entropy change was calculated for all samples for magnetic field change of 1 T and is shown in figure 4.14. The entropy change was calculated according to (2.32). The very large, sharp and narrow peak for the pure $DyCo_2$ compound is due to the first order transition of this compound. The enumerated value of the entropy change according to (2.32) is therefore just rough estimation.

We can see the suppression of the maximum value of the entropy change ΔS_m^{max} with the iron substitution and the $-\Delta S_m^{max}$ amounts 5.0, 1.7 and 1.3 $JK^{-1}.kg^{-1}$ for x = 0.00, 0.01 and 0.03, respectively, for a field change of 1 T. On the other hand, the calculated RCP for a field change of 1 T does not change considerably – we estimated the values of 35, 41 and 35 Jkg^{-1} for 0, 1 and 3% of Fe, respectively. The nearly unchanged RCP reflects the fact that the decrease of ΔS_m maxima is compensated by an increase of the width of the ΔS_m vs T peak. Similar trends with slightly higher ΔS_m values are reported

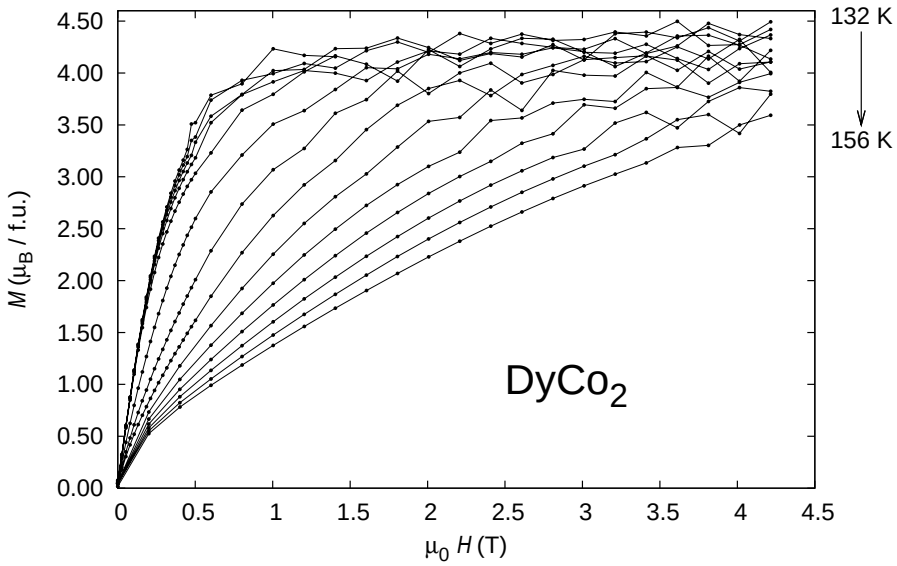

Figure 4.13: The magnetization isotherms of the pure $DyCo_2$ sample. The kinkiness of the magnetization curve at higher field is due to the release of the powder.

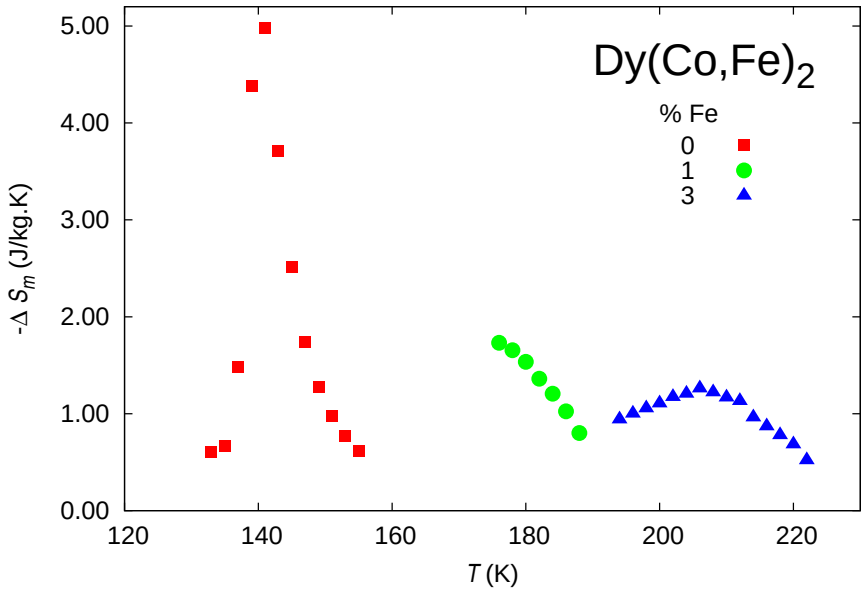

Figure 4.14: The entropy change for the $Dy(Co_{1-x}Fe_x)_2$ system for the magnetic field change from 0 to 1 T. We note that 1 $J.K^{-1}.kg^{-1} \doteq (0.221 + 0.003x)$ $J.K^{-1}.mol^{-1}$.

Table 4.2: The structural and magnetocaloric characteristics of the $Dy(Co_{1-x}Fe_x)_2$ series. We note that 1 $J.K^{-1}.kg^{-1} \doteq (0.221 + 0.003x)$ $J.K^{-1}.mol^{-1}$ (* valid for the field change from 0 to 1 T)

x	a (Å)	T_c (K)	-ΔS (J/K.kg) *	RCP (J/kg)
0.00	7.192	140	4.98	34.8
0.01	7.196	178	∼1.73	41.5
0.03	7.200	210	1.26	35.3

also by Han et al. [33]. The small difference can be explained by the differences in the sample preparation. As in our case, the large value of the entropy change is observed for the pure $DyCo_2$ which is explained as the first order transition effect.

The values of the RCP, the entropy change and the lattice parameter is summarized in Table 4.2. The temperature dependence of the entropy change for the sample with 1% of iron was symmetrically completed in order to enumerate the RCP value.

The obtained value of the entropy change on the studied $Dy(Fe,Co)_2$ and $Gd(Rh,Co)_2$ are comparable with value obtained on other $RECo_2$ system with transition temperature in the same region. Very interesting trend of the maximum entropy change and the transition temperature is in paper of Duc et al. [35]. $Dy(Fe,Co)_2$ and $Gd(Rh,Co)_2$ follow the same general tendency of increasing the entropy change with the decreasing T_c. The values of the entropy change in the systems studied in our work are fairly below the full line of figure 7 in [35] for T_c around 200 K and tend to reach the full line at the room temperature. We take the mentioned figure 7 in [35] and present here as figure 4.15 for easy comparison. We add the value for $Gd(Rh,Co)_2$ to 4.15. We do not have the maximum entropy change for $Dy(Fe,Co)_2$ for field change of 5 T.

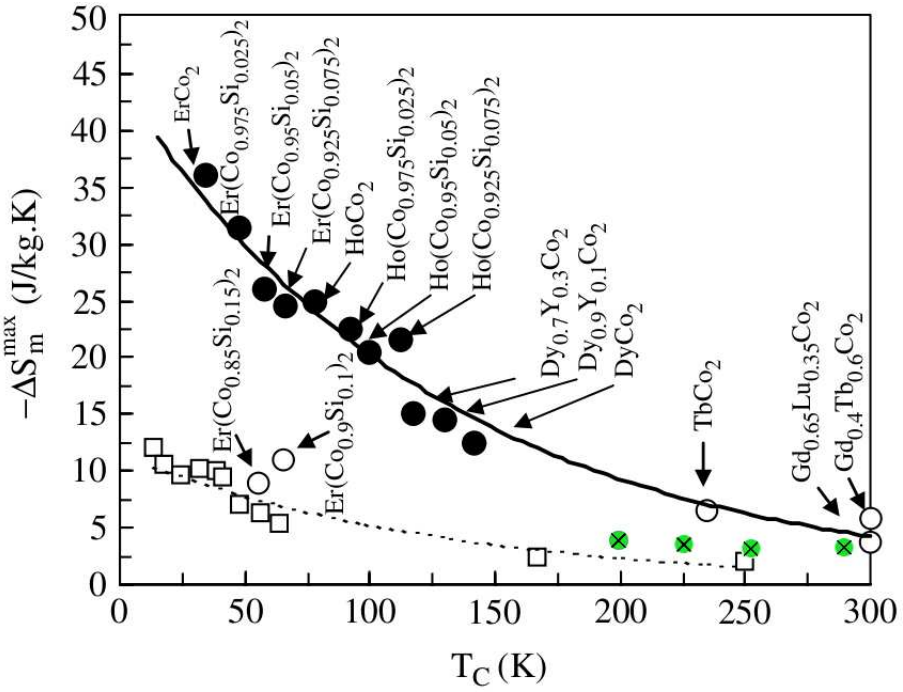

Figure 4.15: The Δ_m^{max} vs. T_c of RECo$_2$ based compounds (open circle - second-order transition; filled circle - first-order transition) and REAl$_2$ based compounds (open squares - second-order transition) taken from [35]. Gd(Rh,Co)$_2$ compounds (crossed circle - second-order transition); The values are obtained for magnetic field change of 5 T.

4.3 Gg-Tb alloys

The Gd-Tb alloys crystallize in a hexagonal structure with the crystallographic space group P6$_3$/mmc. The picture of this structure can be seen in figure 4.16. Concerning the magnetic properties, pure gadolinium undergoes the first magnetic transition from the paramagnetic state to the ferromagnetic state with moment along the c-axis (easy direction) at 293 K. The change of the easy direction from the c-axis to the easy cone takes place at 240 K [36]. Pure terbium has a little more complicated magnetic structure. It undergoes the magnetic transition from the paramagnet to spiral magnetic structure at the temperature of 229 K. The transition from this spiral structure to the ferromagnetic structure appears then at 221 K.

The six samples of $Gd_{1-x}Tb_x$ with x=0.00, 0.10, 0.20, 0.25, 0.30 and 0.40 were prepared. The temperature dependence of the magnetization, $M(T)$, was measured on all samples to find the transition temperature. The obtained curves are shown in figure 4.17. Small piece in elliptical shape of all concentrations was prepared for the magnetization measurement to minimize the influence of the sample shape. The exception is sample of $Gd_{0.9}Tb_{0.1}$ for which the thin ribbon oriented perpendicular to the field was measured. The influence of the sample shape on the temperature dependence of the magnetization is clearly seen in figure 4.17 for this $Gd_{0.9}Tb_{0.1}$ sample. Nevertheless, the data were good

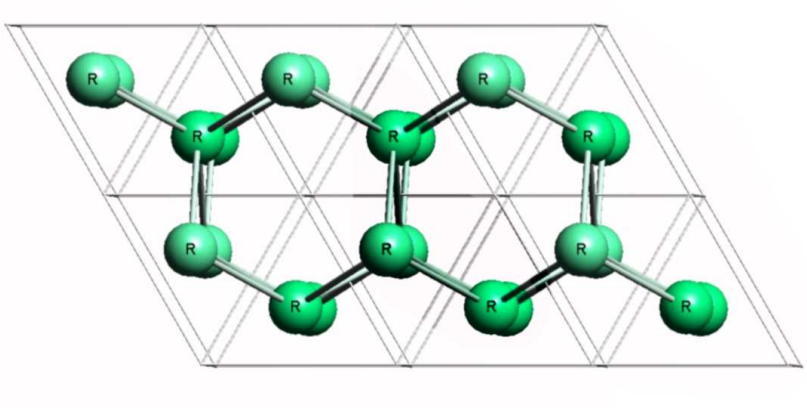

Figure 4.16: The unit cell of the pure Gd, Tb and Gd-Tb alloys. The ratio between the Gd and Tb content change only the lattice parameters.

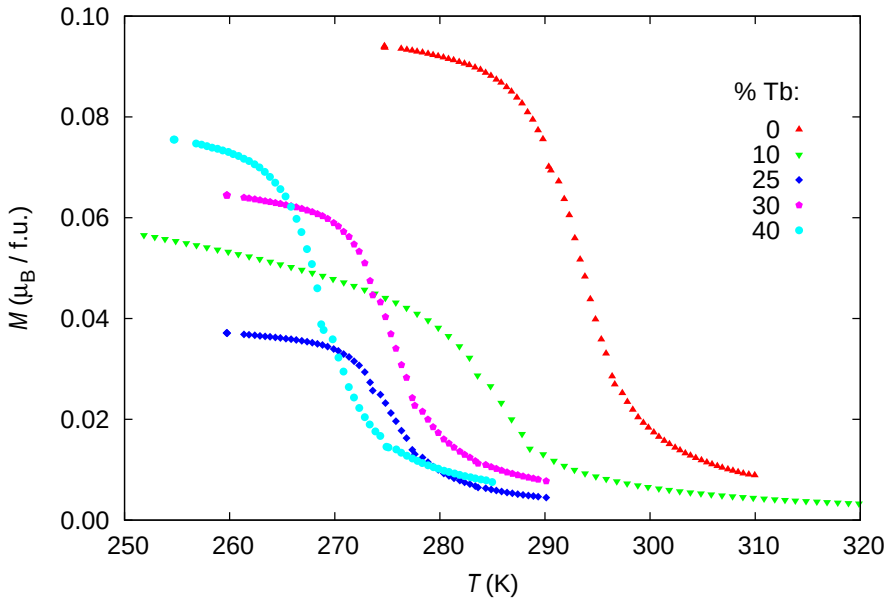

Figure 4.17: The temperature dependence of magnetization for the Gd-Tb series. The curves were measured in magnetic field of about 0.01 T. All curves shown were measured during cooling. The observed hysteresis is negligible and the curves measured during heating will overlay the shown curves.

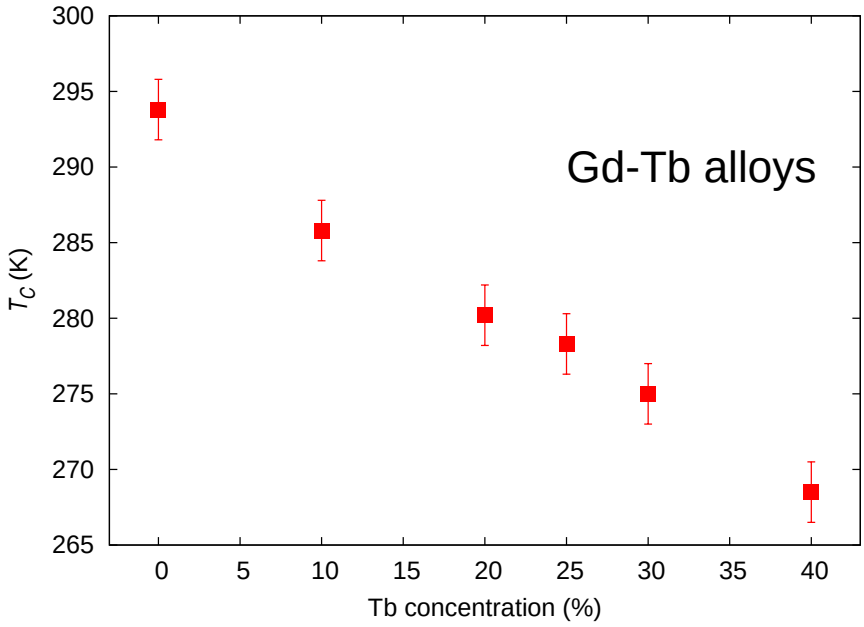

Figure 4.18: The concentration dependence of the transition temperature of the Gd-Tb alloys. The linear decrease is evident.

enough to determine the transition temperature. The temperature dependence of the sample $Gd_{0.8}Tb_{0.2}$ was measured on another instrument (MPMS at Institute of Physic of the AS CR) in different magnetic field (∼0.02 T) and is not shown in figure 4.17. The $M(T)$ measured for $Gd_{0.6}Tb_{0.4}$ and pure Gd measured when cooling and heating show that the hysteresis of Gd-Tb samples is very small and can be neglected. There are kink points on all $M(T)$ curve measured at cooling (at heating the curve was intact). These points are at the same value of magnetization expressed in EMU for all the samples. The origin of these error points is not yet clear to us but the repeating of the error points for all samples at the same value of EMU suggest that it can be an error of the instrument. The transition temperature, derived as the maximum of the first derivative of $M(T)$, can be seen in figure 4.18. There is the linear decrease of the transition temperature with increasing terbium concentration. The linear decrease and obtained values of transition temperatures are in good agreement with previously published data [37, 38].

To test the influence of the sample shape on magnetocaloric effect, the samples were prepared in different sizes and shapes. There was brief overview of the samples shape in the section 3.1. The approximate sample shape for direct measurement is shown in figure 4.19. The proportions of each sample prepared for direct measurement are summarized in Table 4.3. The samples of $Gd_{0.9}Tb_{0.1}$ were also prepared in shapes of a thin (∼0.03 mm) ribbon and as a spiral made from this ribbon for the indirect measurement.

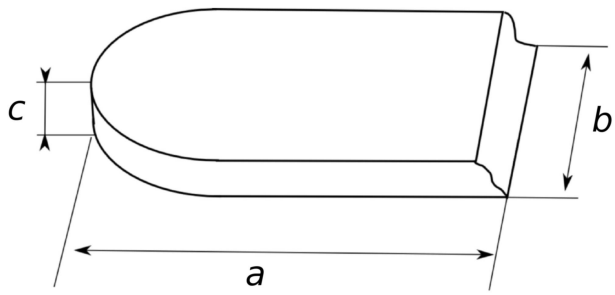

Figure 4.19: The approximate shape of the samples for direct measurement.

Table 4.3: The proportions of the samples used for the direct measurement. The meaning of the a, b and c is explained by figure 4.19.

x	a (mm)	b (mm)	c (mm)	weight (mg)
0.00	10.0	7.7	2.3	999
0.10	9.2	5.1	2.6	630
0.25	5.8	5.2	2.7	531
0.30	7.0	5.0	3.0	843
0.40	6.0	5.0	2.0	272

4.3.1 Magnetocaloric effect in $Gd_{0.9}Tb_{0.1}$

We choose the sample with 10% of Tb for the comparison of the measurement techniques and for determination of the influence of the sample shape. The influence of the sample shape was found out from the measurement of the magnetization isotherms on samples with different shape and in different orientation. The entropy change for each shape is shown in figure 4.20. The results for the bulk, spiral and the ribbon oriented along the field direction is almost the same in the paramagnetic region (on the right from the maximum), but the peaks of entropy change have different width in the ferromagnetic region (on the left from the maximum). The peaks can be ranged by the width in the ferromagnetic region from the widest to the narrowest in this order: ribbon along the field, spiral and bulk. The ribbon oriented perpendicular to the field gives markedly smaller value of the entropy change in the whole studied region what can be attributed to the demagnetization field of the sample. The entropy change for the bulk fits quite well with the value presented by M. Balli et al. [38].

The heat capacity was measured on the bulk sample to compare different measurement techniques. The temperature change from the heat capacity measurement was obtained as a difference between the temperatures at which the entropy measured in field and without the field has the same value (illustrated in figure 2.1). The temperature change can be also calculated from the zero-field heat capacity and the magnetization curves at different temperatures. We enumerate the entropy change according to the equation

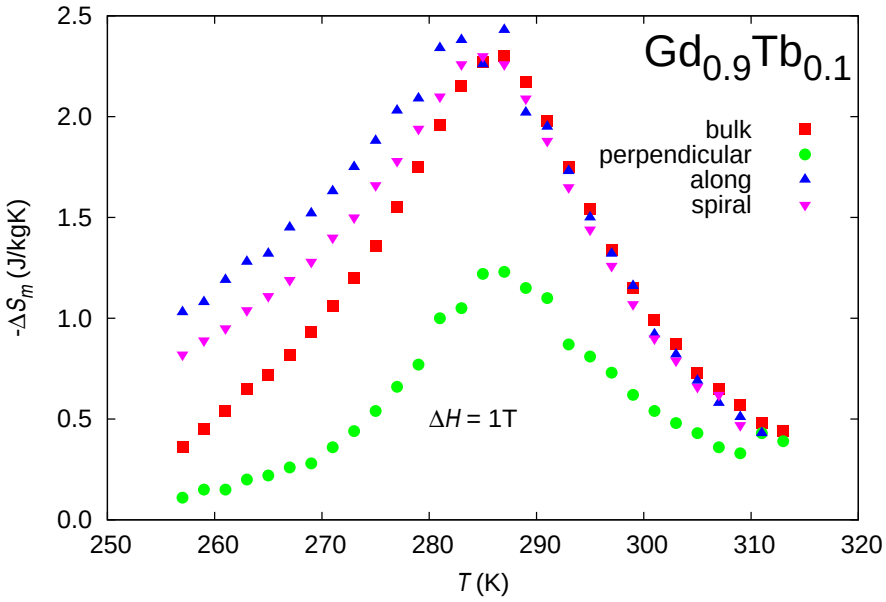

Figure 4.20: The results for the bulk, spiral and the ribbon oriented along the magnetic field direction and perpendicular to the field is shown. The effect of demagnetization field can be clearly seen on the ribbon oriented perpendicular to the magnetic field.

(2.32), then we sum the entropy in zero field and the entropy change. After this we know the entropy in non-zero field and in zero field and then we proceed as in the case of the heat capacity. The comparison is in figure 4.21. The position of maxima is the same for all the three methods. The highest value of the temperature change was obtained by the magnetization measurement followed by the heat capacity measurement. The lowest value of the temperature change was given by the direct measurement. This results is probably more general then only for this samples [39]. Our possible explanation of the lowest value obtained by the direct measurement is the error of interpolation of the very fast sample relaxation.

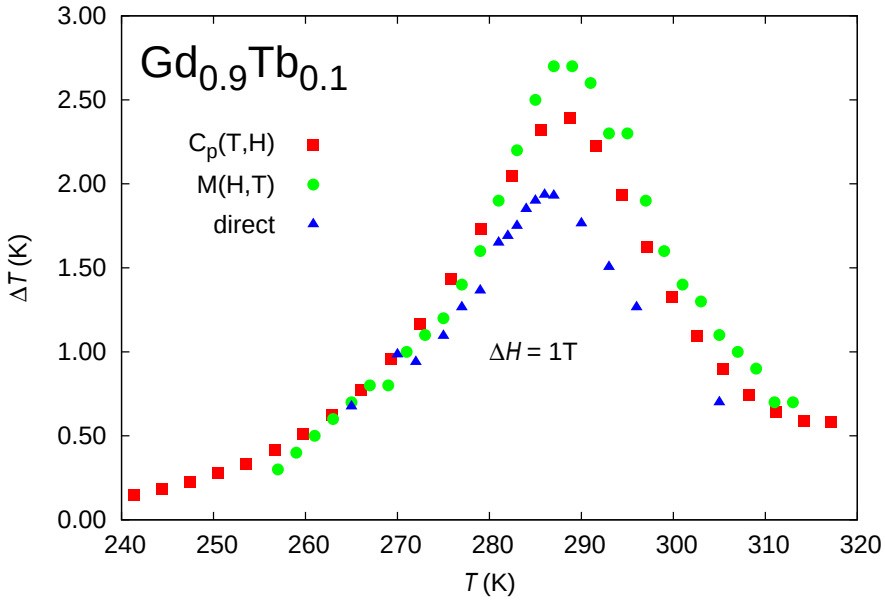

Figure 4.21: The temperature dependence of the temperature change obtained by three different measurement method for the $Gd_{0.9}Tb_{0.1}$ alloy. The magnetization measurement and the heat capacity measurement was measured on the same sample. The direct measurement was realized on different sample due to the instrument needs.

4.3.2 Results for the whole set

The direct measurement was performed to obtain the adiabatic temperature change for the whole set of Gd-Tb alloys. The results are represented in figures 4.22 and 4.23. The positions of the maxima of the peaks correspond, within the experimental error, with the transition temperatures obtained from the indirect measurement $M(T)$ dependencies. It holds for for all samples that the positions of ΔT maximum are at higher temperatures (by about 2 K) when measured at moving out the magnetic field. This shift in the position of the maxima is due to the difference between the heat capacity in the field and out of the field – the change of the thermal energy of the lattice is the same, but the change of the temperature depends on the heat capacity. The values of the maximum ΔT has no general trend and are in the proximity of 2.5 K. The error of the temperature change obtained from the direct method is probably around 30%. We have no exact formula to calculate the error.

The measurement of the temperature change was also measured in different orientations of the sample to the field direction to find out the dependence of the maximum temperature change on the angle between the magnetic field direction and the sample (the side a from figure 4.19). The measurement was performed in the vicinity of the position of the maximum temperature change. The results are figured out in 4.24. It can be clearly seen that the temperature change depends on the field direction. The maximum of the temperature change is swelled when the longest side is along the field direction (0

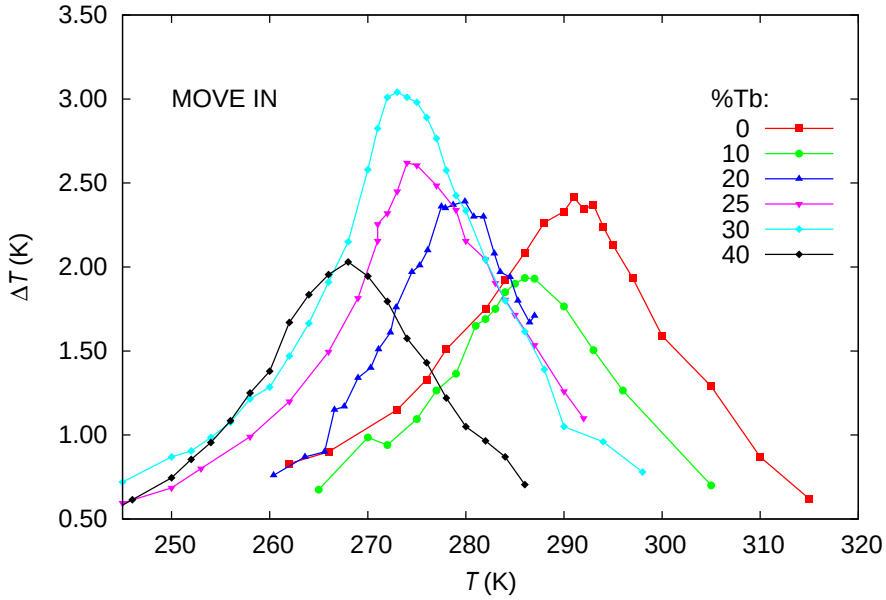

Figure 4.22: The temperature dependence of the temperature change ΔT for the whole set of Gd-Tb alloys. MOVE IN means that the values were obtained when applying the magnetic field. The line in the figure is only to guide the eye.

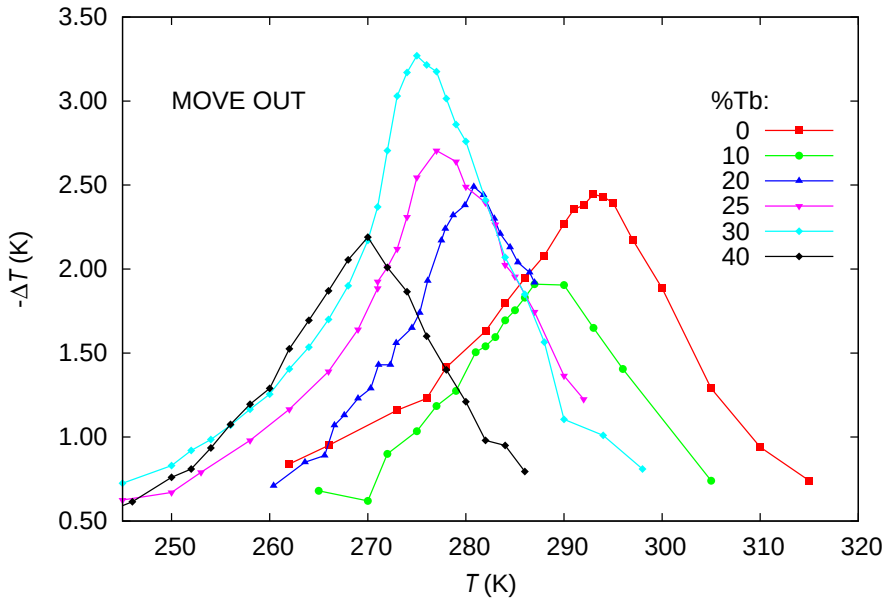

Figure 4.23: The temperature dependence of the temperature change ΔT for the whole set of Gd-Tb alloys. MOVE OUT means that the values were obtained when removing the magnetic field. The line in the figure is only to guide the eye.

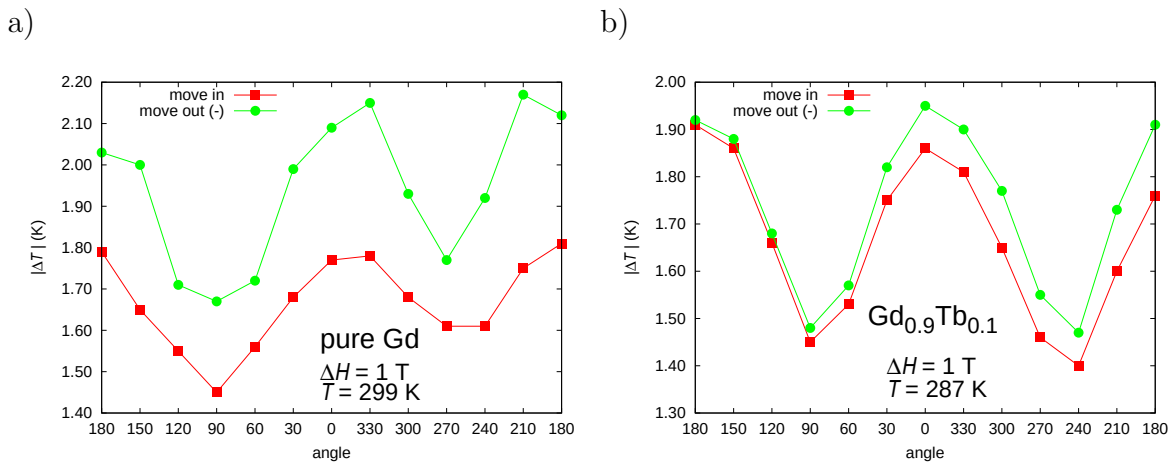

Figure 4.24: The angular dependence of the temperature change of the a) pure Gd; b) $Gd_{0.9}Tb_{0.1}$. The "angle" on the x-axis is the angle between the longest side of the sample (side a in figure 4.19) and the magnetic field direction.

and 180°) and the minimum when the field is perpendicular to the longest side of the sample. We note that the data in figures 4.22 and 4.23 were measured for the sample orientation corresponding to the highest ΔT values. The results obtained from the direct measurement of the orientation dependence are in a good agreement with the results from the indirect measurement (figure 4.20).

We also speculate about the influence of the sample texture on the magnetocaloric effect and on the mechanical properties. The magnetic anisotropy of the Gd-Tb alloys is not so high. We start to investigate the difference between the rolled samples and the bulk samples by the x-ray diffraction measurement on the rolled thin ribbon of $Gd_{0.9}Tb_{0.1}$ and on the piece cut from the not-rolled ingot of $Gd_{0.8}Tb_{0.2}$. The results are showed in figure 4.25. The different ratio between the peaks suggest the existence of the texture on the sample. The detailed study of the texture is under progress an will continue.

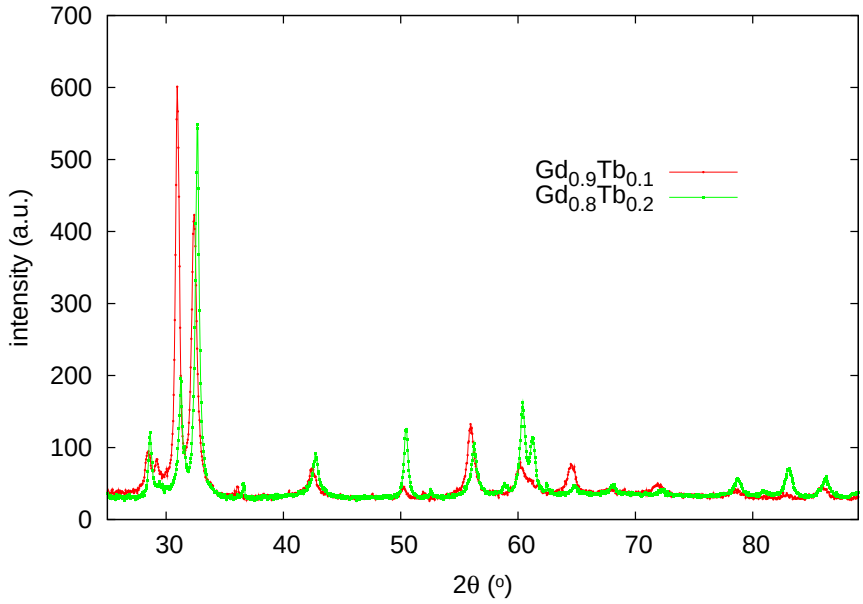

Figure 4.25: The difractograms of rolled $Gd_{0.9}Tb_{0.1}$ and not-rolled $Gd_{0.8}Tb_{0.2}$. The shift of the peaks position is due to the different concentration. The different ratio between the peaks suggest the existence of the sample texture.

Chapter 5

Conclusions

We have performed detailed magnetization measurement of the DyNiAl single crystal and compared obtained results with the previous papers. Our data reveal a strong anisotropy of the magnetocaloric effect in DyNiAl. The maximum entropy change reaches the value of 14 and 22 $Jkg^{-1}K^{-1}$ for the field change of 2 and 5 T applied along the c-axis, respectively, and is significantly enhanced compared to polycrystalline data. Smaller effect and rather complex behaviour is observed for the field applied along the a-axis. The entropy change is mostly due to the ordering of the ferromagnetic component at T_c. The entropy change related to the order of the antiferromagnetic component at T_1 is relatively small and is recorded only when the field is applied perpendicular to the c-axis.

We have studied the magnetocaloric effect in $Gd(Co,Rh)_2$ and $Dy(Co,Fe)_2$ series. The substitution in both series allows precise tuning of the ordering temperature between 150 and 350 K. The Rh substitution in $Gd(Co,Rh)_2$ leads to a decrease of the ordering temperature and a small increase of magnetocaloric effect. The Fe substitution in $Dy(Co,Fe)_2$ causes disappearance of the first-order type transition already for 1% of Fe with a simultaneous strong increase of the ordering temperature. The $Dy(Co,Fe)_2$ compounds exhibit slightly larger magnetocaloric effect than the $Gd(Co,Rh)_2$ compounds at the same temperature.

We gave grate attention to the Gd-Tb alloys. The sample with different Tb concentrations and shapes were prepared. We were able to change fluently the transition temperature by changing the Tb concentration. The magnetization measurement showed the influence of the shape on the entropy change. The thin ribbon oriented perpendicular to the field gave remarkably smaller value of the entropy change then the other samples. The best results gives the thin ribbon oriented along the field direction. The direct measurement of the temperature change on gradually rotating samples confirm this conclusion. The Gd-Tb alloy is a good magnetocaloric material with suitable mechanical properties. The Gd-Tb alloy is the best candidate for the real application among the materials studied in this work.

The influence of the magnetic anisotropy and the sample texture on the magnetocaloric

effect in Gd-Tb alloys has to be further investigated. The mechanical properties of the Gd-Tb alloys have to be improved to allow preparation of good pieces in the desired shape. The influence of the annealing on the sample texture and mechanical properties, study of samples with other Tb concentration and the improvement and better managing of the direct measurement technique can be subject of further work.

Bibliography

[1] Giauque W. F., MacDougall D. P.: Phys. Rev. 43 (1933) 768 - 768.

[2] A. O. Pecharsky, K. A. Gschneidner, Jr.: Journal of Applied Physics 93 (2003) 8.

[3] A. O. Pecharsky, K. A. Gschneidner, Jr.: Journal of Magnetism and Magnetic Materials 167 (1997) L179-L184.

[4] A. O. Pecharsky, K. A. Gschneidner, Jr.: Physical Review Letters 78 (1997) 23.

[5] K. Fukamichi, A. Fujita, S. Fujieda: Journal of Alloys and Compounds, Volumes 408-412, 9 February 2006, Pages 307-312.

[6] S. Fujieda, A. Fujita, K. Fukamichi, N. Hirano, S. Nagaya: Journal of Alloys and Compounds, Volumes 408-412, 9 February 2006, Pages 1165-1168.

[7] S. Fujieda, Y. Hasegawa, A. Fujita, K. Fukamichi: Journal of Magnetism and Magnetic Materials, Volumes 272-276, Part 3, May 2004, Pages 2365-2366.

[8] L. Song, G.F. Wang, Z.Q. Ou, O. Haschaolu, O. Tegus, E. Brück, K.H.J. Buschow: Journal of Alloys and Compounds 474 (2009) 388–390.

[9] H. Wada, T. Morikawa, K. Taniguchi, T. Shibata, Y. Yamada, Y. Akishige: Physica B 328 (2003) 114–116.

[10] O. Tegus, E. Bruck, L. Zhang, Dagula, K.H.J. Buschow, F.R. de Boer: Physica B 319 (2002) 174–192.

[11] G. Ehlers, H. Maletta: Phys. B 101 (1996) 317.

[12] P. Javorský, N.C. Tuan, M. Diviš, L. Havela, P. Svoboda, V. Sechovský, G. Hilscher: J. Magn. Magn. Mat. 140-144 (1995) 1139.

[13] Niraj K. Singh, K.G. Suresh, R. Nirmal, A.K. Nigam, S.K. Malik: Journal of Magnetism and Magnetic Materials 302 (2006) 302–305.

[14] N. K. Singh, K. G. Suresh, R. Nirmala, A. K. Nigam, S. K. Malik: Journal of Applied Physics 101 (2007) 093904.

[15] N.K. Singh, K.G. Suresh, R. Nirmala, A.K. Nigam, S.K. Malik: Journal of Applied Physics 99 (2006) Art. No. 08K904.

[16] A.L. Lima, A.O. Tsokol, K.A. Gschneidner, Jr., V.K. Pecharsky, T.A. Lograsso, and D.L. Schlagel: Phys. Rev. B 72 (2005) 024403.

[17] M. Zou, Y. Mudryk, V. Pecharsky, K. Gschneidner, D. Schlagel, and T. Lograsso: Phys. Rev. B 75 (2007) 024418.

[18] A.L. Lima, K.A. Gschneidner, Jr. and V.K. Pecharsky: Journal of Applied Physics 96 (2004) 2164.

[19] L. Li , K. Nishimura, D. Tamei, K. Mori: Solid State Communications 145 (2008) 427–431.

[20] W.Q. Ao, J.Q. Li, F.S. Liu, Y.X. Jian: Solid State Communications 219–222 (2007) 141.

[21] Z. Gu, Bo Zhou, J. Li, W Ao, G. Cheng, J. Zhao: Solid State Communications 141 (2007) 548–550.

[22] D. Vasylyev, J. Prokleška, J. Šebek, V. Sechovský: Journal of Alloys and Compounds 394 (2005) 96-100.

[23] J.Y. Zhang, J. Luo, J.B. Li , J.K. Liang, Y.C. Wang, L.N. Ji, Y.H. Liu , G.H. Rao: Solid State Communications 143 (2007) 541–544.

[24] Charles Kittel: Úvod do fyziky pevných látek, Academia, Praha 1985.

[25] A.V. Andreev, N.V. Mushnikov, T. Goto, J. Prchal: Physica B 346-347 (2004) 201.

[26] J. Prchal , A.V. Andreev, P. Javorský, F. Honda, K. Jurek: J. Magn. Magn. Mat. 272-276 (2004) e419.

[27] J. Prchal, P. Javorský, K. Prokeš, B. Ouladdiaf, A.V. Andreev: Physica B 385-386 (2006) 346-348.

[28] Rodriguez-Carvajal, J.:Physica B.(1993), 192, 55.

[29] L. Morellon, C. Magen, P.A. Algarabel, M.R. Ibarra, C. Ritter: Appl. Phys. Lett. 79 (2001) 1318.

[30] E. Gratz and A. S. Markosyan: J. Phys.: Condens. Matter 13 (2001) R385.

[31] M. Balli, D. Fruchart, D. Gignoux: J. Alloys and Compounds 455 (2008) 73.

[32] D. H. Wang, S. L. Tang, H. D. Liu, W. L. Gao, Y. W. Du: Intermetallics 10 (2002) 819.

[33] Zhida Han, Zhenghe Hua, Dunhui Wang, Chengliang Zhang, Benxi Gu, Youwei Du: J. Magn. Magn. Mat. 302 (2006) 109.

[34] J.Y. Zhang, J. Luo, J.B. Li , J.K. Liang, Y.C. Wang, L.N. Ji, Y.H. Liu , G.H. Rao: Solid State Communications 143 (2007) 541–544.

[35] N.H. Duc, D.T. Kim Anh, P.E. Brommer: Physica B 319 (2002) 1.

[36] R.L. Smith, W.D. Corner and B.K. Tanner: J. Magn. Magn. Mat. 20 (1980) 265-270.

[37] M. Balli, D. Fruchart, D. Gignoux, E.K. Hlil, S. Miraglia, P. Wolfers: Journal of Alloys and Compounds 442 (2007) 129–131.

[38] M. Balli, D. Fruchart, D. Gignoux, S. Miraglia, E.K. Hlil, P. Wolfers: Journal of Magnetism and Magnetic Materials 316 (2007) e558–e561.

[39] J. Kamarád, O. Heczko: private comunications.